THE EFFECT OF HACE1 ON RAR PROTEIN STABILITY

A Thesis
Submitted to the
Temple University Graduate Board

In Partial Fulfillment
Of the Requirements for the Degree
MASTER OF SCIENCE

By
Erin J. Payne
August, 2011

Thesis Approval:

Kenneth J. Soprano, Ph.D, Thesis Advisor, Microbiology & Immunology
Alexander Y. Tsygankov, Ph.D., Microbiology & Immunology
Earl Henderson, Ph.D., Microbiology & Immunology

ABSTRACT

The Effect of HACE1 on RAR Protein Stability

Erin Payne

Master of Science

Temple University, 2011

Master's Advisory Committee Chair: Kenneth J. Soprano, Ph.D.

All-trans retinoic acid (RA), as a ligand for retinoic acid receptors (RAR) and retinoid X receptors (RXR), modulates their transcriptional activity. The AF-1 and AF-2 domains mediate the transcriptional activity. The ligand dependent activation of the AF-2 domain by RA is well understood to involve chromosome decompaction in the presence of ligand with the aid of coactivators. The mechanism of the ligand independent action of the AF-1 domain is less clear. The AF-1 domain of RARs may be regulated by interacting proteins such as HACE1.

In vitro and *in vivo* studies in our lab have shown that HACE1 interacts with RARα_1, - β_1, -β_2, -β_3, and –γ_1 at the variable AF-1 domain. Transactivation studies have shown that HACE1 represses RA dependent transcriptional activity of RARγ_1, but not RARβ_3 and RARα_1. Our original hypothesis proposed that HACE1 represses RAR transcriptional activity by inhibiting RA-dependent degradation of RARs. Current data confirms previous observations that the half life of RARβ_3 is shortened in the presence of RA, compared to a vehicle control. Protein stability assays show that HACE1 does not

have an effect on degradation of RARβ_3 and RARγ_1; however, it increases the ligand independent degradation of RARα_1.

This data suggests the A/B domain of RARγ_1 recruits HACE1 for binding which results in transcriptional repression. Also, in a separate mechanism, the A/B domain of RARα_1 binds to HACE1 which then accelerates its degradation in a ligand independent manner. The mechanisms behind these novel roles of HACE1 will need to be studied further and may help in understanding the method of AF-1 transcactivation function.

ACKNOWLEDGEMENTS

I would first like to thank my advisors Dr. Kenneth J. Soprano and Dr. Dianne R. Soprano for their encouragement and intelligence in guiding me through my training. I would also like to thank my committee members, Dr. Alexander Tsygankov and Dr. Earl Henderson, for their advice on my project over the years.

I would like to acknowledge all the members of the Soprano labs: Dorret Garner, Zhang Zhenping, Dr. Thais Acquafreda, Dr. Maria Radu, Dr. Bryan Teets, Dr. Jianhua Zhao, Evelyn Sirisani, Brandy Pickens, and Fang Wang. They all provided welcome feedback on my project and friendship. Other members of the Microbiology and Immunology department also lent their friendship and company, especially Rebecca Hartzell.

Thank you to all my family and friends who encouraged me in my studies and reminded me of life outside them. And to Rinna Hoffman, who revives me daily.

TABLE OF CONTENTS

Page

LIST OF ABBREVIATIONS

ADH	alcohol dehydrogenase
AF	activation function
ANOVA	analysis of variance
ATCC	American Type Culture Collection
ATP	adenosine 5’-triphosphate
BP	binding protein
CDK	cyclin-dependent kinase
cDNA	complementary DNA
CRABP	cellular retinoic acid binding protein
CRBP	cellular retinol binding protein
DBD	DNA binding domain
ddH_2O	distilled deionized water
DMEM	Dulbecco’s modified Eagle’s medium
DNA	deoxyribonucleic acid
dNTP	deoxribonucleotide triphosphate
DR	direct repeat
Eth	ethanol
FBS	fetal bovine serum
g	standard acceleration of gravity
GAPDH	glyceraldehydes 3-phosphate dehydrogenase
H	helix

HACE1	HECT domain and ankyrin repeat containing E3 ubiquitin-protein ligase
HDAC	histone deacetylase
HECT	homologous to E6-AP C-terminus
hr	hour
HSV-TK	Herpes simplex virus thymidine kinase
kD	kilodalton
L	liter
LBD	ligand binding domain
LF	long form
LRAT	lecithin:retinol acetyltransferase
Luc	Luciferase
M	molar
MAPK	mitogen-activated protein kinase
mg	milligram
min	minute
mL	milliliter
mM	millimolar
mRNA	messenger ribonucleic acid
MW	molecular weight
N-CoR	nuclear receptor corepressor
NMR	nuclear magnetic resosance
NTD	N-terminal domain

PAGE	polyacrylamide gel electrophoresis
PCR	polymerase chain reaction
PLB	passive lysis buffer
PMSF	phenylmethylsulphonyl fluoride
PolII	RNA polymerase II
pTK-RL	renilla luciferase vector
RA	all-*trans* retinoic acid
RALDH	retinal dehydrogenase
RAR	retinoic acid receptor
RARE	retinoic acid response element
RARE-luc	RARE firefly luciferase reporter vector
RBP	retinol binding protein
RDH	retinoid dehydrogenase
RE	retinol equivalent
RLU	relative luciferase units
RNA	ribonucleic acid
RXR	retinoid X receptor
RXRE	retinoid X response element
SDR	short-chain dehydrogenase/reductase
SDS	sodium dodecyl sulfate
SF	short form
SMRT	silencing mediator for RAR and TR
TEMED	N, N, N’, N’-tetramethylene diamine

TFB	transformation buffer
Ub	ubiquitin
VAD	vitamin A deficiency
µg	microgram
µL	microliter
µM	micromolar

LIST OF TABLES

Page

LIST OF FIGURES

Page

CHAPTER 1
INTRODUCTION

I. Vitamin A and Retinoids

Vitamin A is a required nutrient involved in various biological processes. Humans are unable to synthesize vitamin A so it must be ingested from outside plant or microorganism sources. Commonly, these sources include red meat, orange or leafy vegetables, milk, and commercial supplements. Once ingested, its metabolic derivatives are involved in differentiation, reproduction, growth, vision, and immune function. The most active form of vitamin A is all-trans-retinoic acid (RA). For night vision, 11-cis retinal is the active form. Collectively, the metabolic derivatives and synthetic analogs of vitamin A are called retinoids. All forms of vitamin A share a similar structure containing a β-ionone ring, a conjugated side chain, and a polar terminal group (Figure 1.1).

Due to its many essential functions, vitamin A deficiency (VAD) can affect multiple systems in an individual. The symptoms of VAD range in severity from dry skin and fatigue to reduced growth, vision, or immune function. Neurological symptoms may also manifest in children. Conversely, an overdose of vitamin A may cause vomiting, anorexia, bone fragility, or death. The recommended daily amount varies by sex and age, but an adult should be ingesting no more than 5000 RE per day. The elderly, people with liver disease, or pregnant women should limit intake to 2000 RE per day (Griffith, 1998).

Vitamin A is most commonly ingested as carotenoids or retinyl esters. Carotenoids are synthesized by plants and many microorganisms. Plant sources of carotenoids can often be identified by their yellow, orange, or red pigmentation such as carrots and sweet potatoes. Secondary sources of carotenoids can be obtained through

eating animal tissue containing stored retinoids. The other major dietary source of vitamin A is retinyl esters. These are present in many dairy products in industrialized countries due to commercial fortifications.

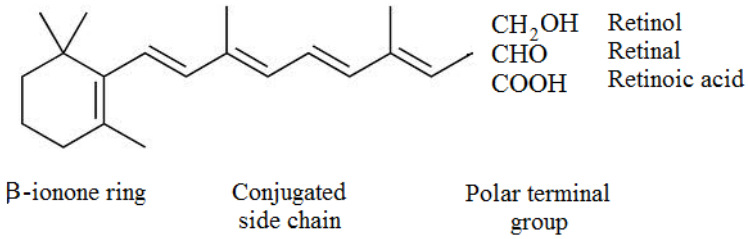

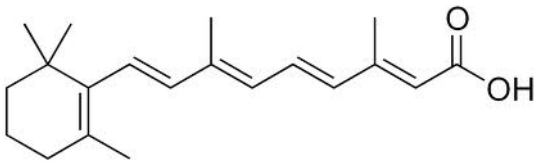

All-*trans* retinoic acid

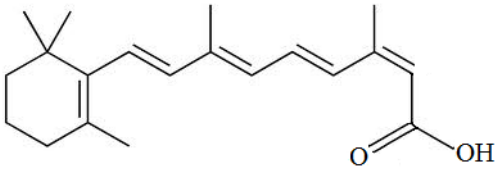

11-*cis* retinoic acid

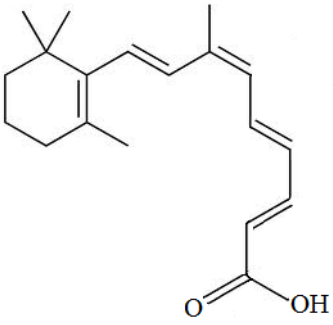

9-*cis* retinoic acid

Figure 1.1: Retinoid structures.

Metabolism of RA

Once ingested, carotenoids are absorbed into enterocytes of the small intestine by passive diffusion. From there, symmetrical or asymmetrical cleavage may occur to produce retinal or β-apocarotenals. Retinal is further reduced to retinol in the intestine. Retinyl esters are converted to retinol in the intestinal lumen before it is taken up by enterocytes. Retinol binds to cellular retinol-binding protein type II (CRBP-II) in enterocytes for re-esterification with long chain fatty acids by lecithin:retinol acyl transferase (LRAT) (Herr and Ong, 1992).

Most retinyl esters are secreted into the intestinal lymph from enterocytes as part of chylomicrons (Blomhoff *et al*, 1990). Unesterified retinol may be secreted into portal circulation (Harrison, 2005). Hepatocytes take up retinyl esters from circulating chylomicron remnants when chylomicrons are hydrolyzed. Retinol binds with retinol binding protein (RBP) at the endoplasmic reticulum for translocation to the Golgi complex. Retinol bound to RBP is then secreted into the plasma (Ronne *et al*, 1983). If not bound for plasma secretion, retinol may enter perisinusoidal stellate cells for storage in the liver, mostly in the esterified form. Kidneys, lungs, and intestines may also store retinyl esters (Nagy *et al*, 1997; Blomhoff and Wake, 1991).

Most circulating retinol is recycled into the plasma by the cells that take it up (Green and Green, 2003; Cifelli *et al*, 2005). A small amount of it is metabolized or degraded within cells. Retinol circulates in the plasma bound to RBP; however, RBP is not required for retinol to enter most tissues (Quadro *et al*, 2003). Other retinoids also circulate in the plasma bound to albumin at lower concentrations than retinol. Circulating carotenoids are bound to lipoproteins due to their fat solubility.

While multiple retinoids may be taken from the plasma into a target cell to form active metabolites, the major reaction within cells for this process converts all-*trans* retinol to all-*trans* retinoic acid. Cytosolic medium-chain alcohol degydrogenases (ADH) and membrane-bound short-chain dehydrogenase/reductases (SDR) oxidize all-*trans* retinol to all-*trans* retinal. All-*trans* retinol bound to CRBP-I is directed to SDRs for oxidation, and the unbound form is oxidized by ADHs (Everts *et al*, 2005). Following this rate-limiting step, several retinal dehydrogenases (RALDH) are responsible for oxidizing retinal to retinoic acid (Figure 1.2).

Turnover of retinol and retinoic acid within cells is necessary to maintain appropriate levels within cells and tissues. CYP26A1, CYP26B1, and CYP26C1, which are cytochrome p450 enzymes, are known to degrade retinoic acid (Reijntjes *et al*, 2004). This process is regulated by cellular retinoic acid binding protein type I (CRABP-I) (Boylan and Gudas, 1992).

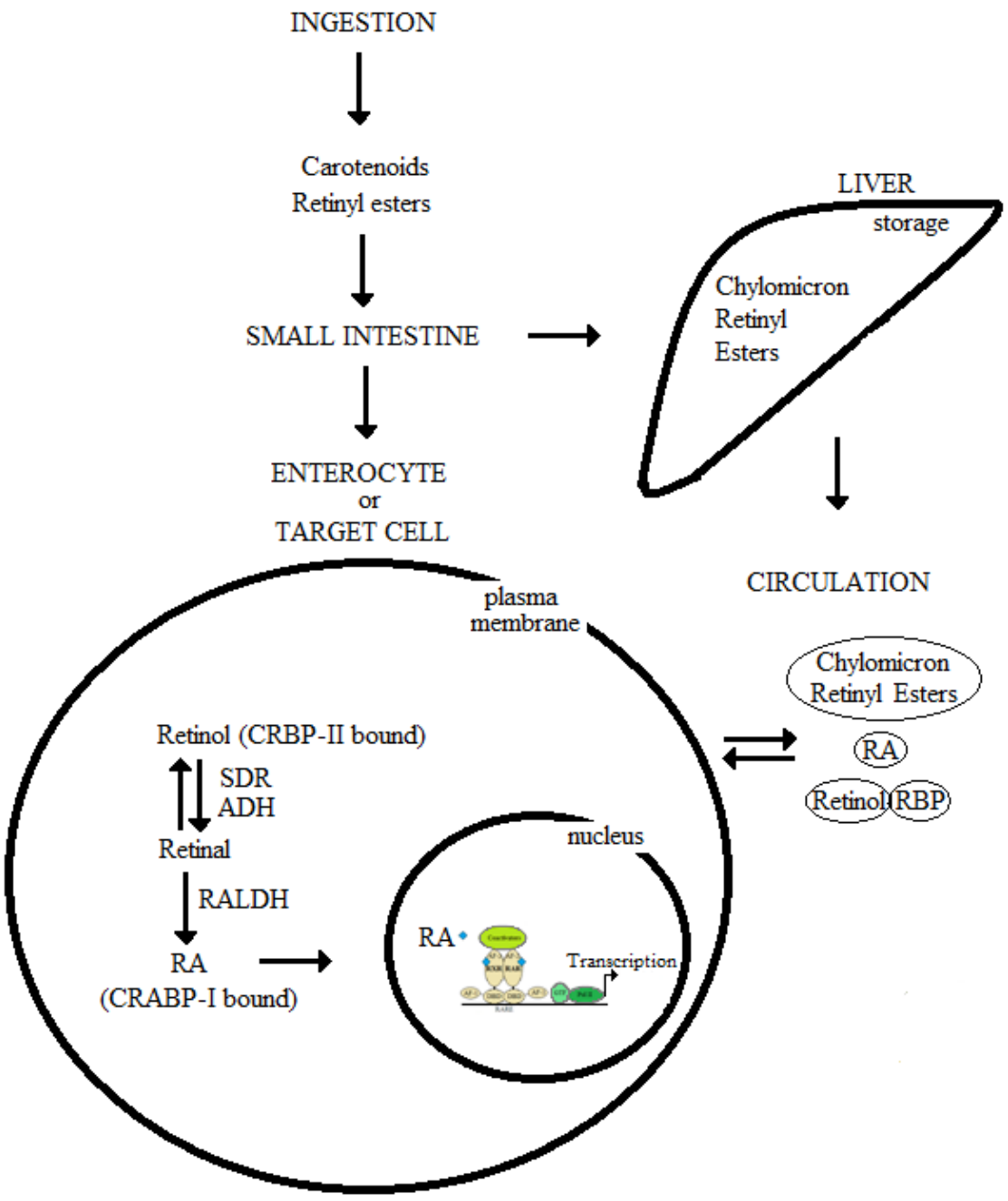

Figure 1.2: Metabolism of RA. Adapted from Fields AL *et al*, 2007.

II. Molecular Mechanisms of RA Function

RA function is mediated by both transcriptional and non-genomic molecular mechanisms. Its effects are often mediated by RARs and RXRs.

Transcriptional Mechanisms of RA Function

Retinoic acid exerts its transcriptional effects through two classes of nuclear receptors, retinoic acid receptors (RAR) and retinoid X receptors (RXR). These two receptors form a heterodimer that interacts with a retinoic acid response element (RARE) in the promoter of specific genes. RA is a ligand for these receptors.

RARs and RXRs heterodimerize on RAREs of target genes. In the absence of ligand, AF-2 recruits corepressors such as NCoR/SMRT that have histone deacetylase activity. These HDACs help to maintain compacted chromatin, preventing transcriptional machinery from accessing the gene (Figure 1.3).

When RA binds to the LBD of RAR, a major conformational change occurs. The corepressors are released from the AF-2 and coactivators are recruited. These coactivators are histone acetyltransferases, histone methyltransferases, and DNA-dependent ATPases that aid in chromatin decompaction (Lefebvre *et al*, 2005; Rosenfeld *et al*, 2006). Coactivators bind at a LXXLL motif forming a hydrophobic cleft after the RA-induced conformational change (Nettles and Green, 2005). Acetyl and methyl groups are added to histone proteins to weaken the interaction with nucleosomal DNA (Aranda and Pascual, 2001). DNA-dependent ATPases move nucleosomes so that genes are exposed to general transcription factors (Narlikar *et al*, 2002).

Following decompaction, coactivators are released so RNA Polymerase II (Pol II) and general transcription factors can access the target gene and initiate transcription (Dilworth and Chambon, 2001). The general transcription factor TFIIH complex can interact with the RARs on the DNA. Cyclin H binds to the AF-2 region, and the AF-1 region is phosphorylated by cdk7 following a conformational change (Bour *et al*, 2005a). RAR and RXR degradation by the proteasome follows in order for transcription to proceed (Figure 1.3; Bour *et al*, 2007).

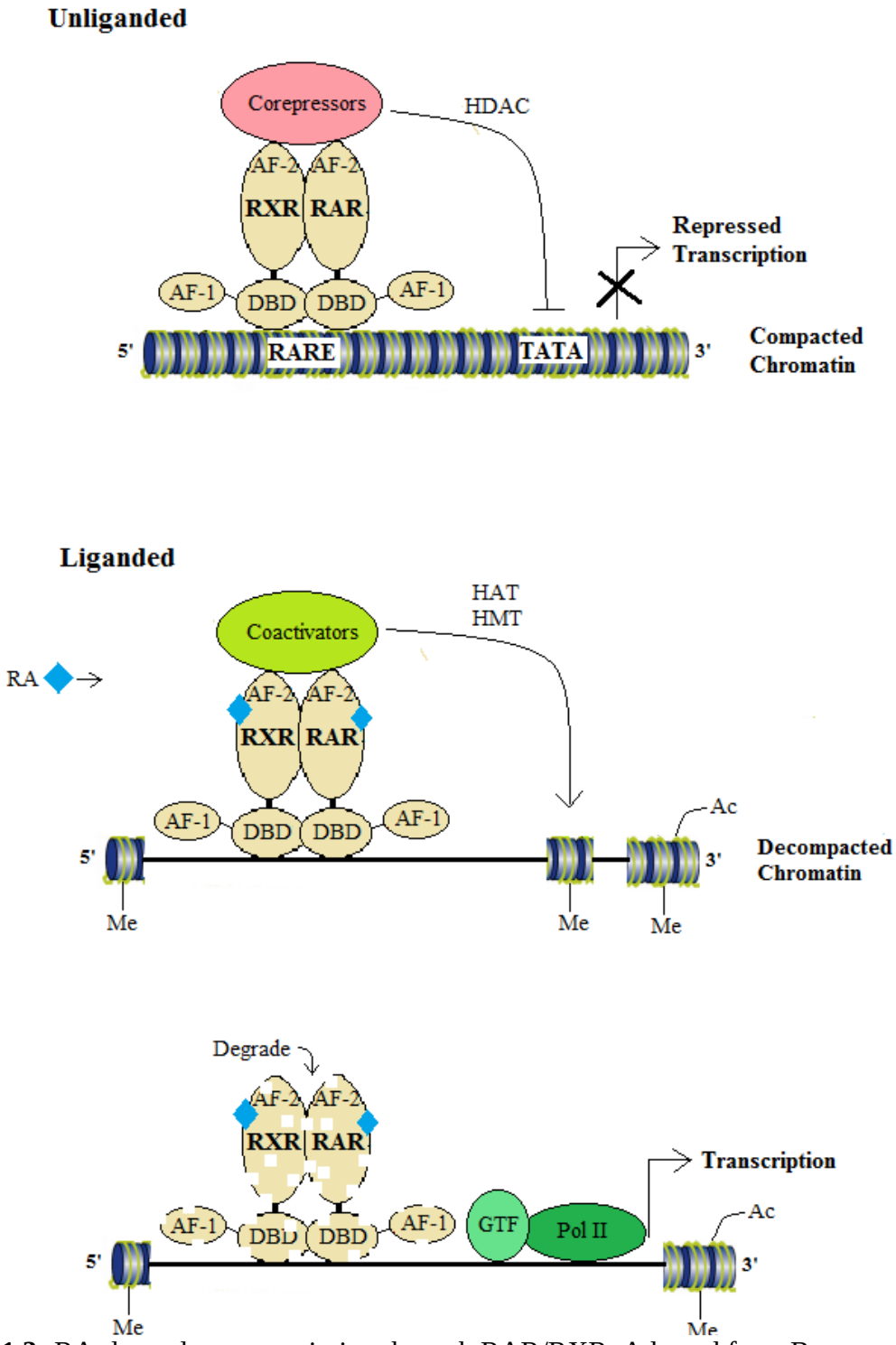

Figure 1.3: RA-dependent transcription through RAR/RXR. Adapted from Bour *et al*, 2007.

Non-genomic Mechanisms of RA Function

In addition to its genomic effects, RA also mediates gene transcription through signaling pathways as non-genomic effects. Many genes sensitive to RA do not contain a recognizable RARE such as PEPCK and c-Fos (Lee *et al*, 2002; Cañón *et al*, 2004). PEPCK gene transcription is enhanced by phosphorylation and activation of ATF-2 from the p38β pathway. RA influences this by activating the p38β pathway through phosphorylation (Lee *et al*, 2002). RA also stimulates CREB and ERK1/2 signaling cascades through activation by phophorylation leading to c-Fos expression and neuronal differentiation (Cañón *et al*, 2004). The signaling pathways regulated by RA appear to differ by cell type (Masia *et al*, 2007; Dey *et al*, 2007; Gupta *et al*, 2008). RA activation by phosphorylation is abolished when appropriate kinase inhibitors are present but not when transcriptional or translational blocking agents are used (Dey *et al*, 2007; Chen and Napoli, 2008). This indicates that the RA effect is indeed propagated through signal pathways instead of through transcriptional regulation.

RARs have been shown to interact with PI3K and SRC, two signaling pathway proteins also regulated by RA (Masia *et al*, 2007; Dey *et al*, 2007). In addition, RARs may localize to the plasma membrane where they can directly interact with signaling pathway proteins (Dey *et al*, 2007; Chen and Napoli, 2008). This evidence indicates that RARs may mediate the non-genomic effects of RA. Furthermore, this phenomenon has already been shown with another steroid/thyroid hormone nuclear receptor superfamily member, ER (For review, see Acconcia and Kumar, 2006).

Retinoic Acid Receptors

There are three subtypes of RARs known as RARα, RARβ, and RARγ. There are two isoforms each of RARα and RARγ that are denoted by number such as $RAR\alpha_1$. There are four isoforms of RARβ, named in a similar manner. The three subtypes of RARs are coded for by three distinct genes which are conserved across species. The isoforms of each subtype originate from alternative splicing and differential promoter usage of the genes. The isoforms differ from others of the same subtype at the N-terminal region. All RAR isoforms may heterodimerize with RXRs. The two ligands known to activate RARs are all-*trans* RA and 9-*cis* RA. All-*trans* RA has been implicated in many transcriptional effects of RARs while the role of 9-*cis* RA is less clear. Generally, RARα is expressed ubiquitously. RARβ and -γ have differential expression across tissues and development (Dollé, 2009).

Retinoid X Receptors

There are also three subtypes of RXRs and two isoforms for each subtype. They are named in a manner consistent with RAR naming. The three subtypes of RXR originate from three distinct genes. The only known ligand for RXR is 9-*cis* RA (Soprano *et al*, 2004). Unlike RARs, RXRs may homodimerize and bind to retinoid X responsive elements (RXRE) in addition to RAREs. Generally, the ligand activation of RXR is overruled by a liganded partner RAR (Germain *et al*, 2002).

RARE

The RAR/RXR heterodimer binds to target genes at a region known as the RARE. These are often, but not exclusively, found in the promoter region of a target gene. The consensus motif of RAREs is a direct repeat of PuG(G/T)TCA separated by one (DR1), two (DR2), or 5 (DR5) nucleotides (Leid *et al*, 1992). For DR2 and DR5 RAREs, the RAR occupies the 3' element, and the RXR occupies the 5' element. For DR1 RAREs, the orientation of the heterodimer is reversed (Kurokawa *et al*, 1995).

III. Structure and Function of RAR and RXR

RARs and RXRs belong to the steroid/thyroid hormone nuclear receptor superfamily which is characterized by a common structure. Members of this superfamily have five or six functionally distinct domains, termed A through F (Figure 1.4). At the N-terminus, the AB region contains a ligand-independent transactivation function (AF-1). The most conserved C region contains the DNA binding domain (DBD) characterized by a pair of zinc fingers. The D domain is the hinge region connecting domains C and E. The E domain contains a ligand-dependent transactivation function (AF-2) and a corresponding ligand binding domain (LBD). It also contains the dimerization surface and surfaces for the binding of coactivators and corepressors. The F domain, present in RARs but not RXRs, has an unknown function (Soprano *et al*, 2004).

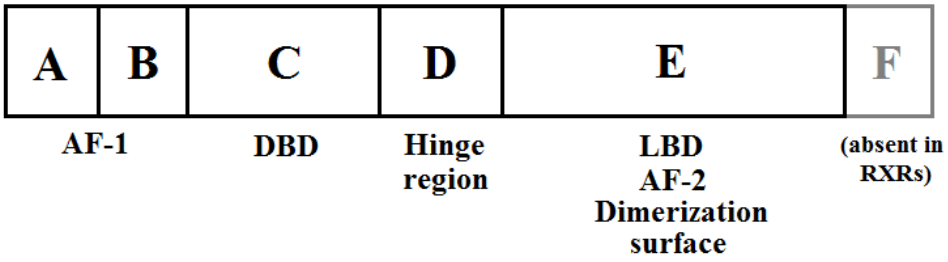

Figure 1.4: Structural domains of RARs and RXRs.

C domain

The C domain is the most conserved region across RARs and RXRs. It contains the DBD composed of two type-II zinc fingers and a C-terminal extension. Each zinc finger is an α-helical structure bound to a zinc ion in a tetrahedral arrangement due to interactions with four cysteines. The two zinc fingers are held perpendicular to each other by hydrophobic interactions. The structure was elucidated by nuclear magnetic resonance and crystallography (Lee *et al*, 1993).

Each partner of the RAR/RXR heterodimer interacts with a half site of a RARE at the DBD. Once zinc finger of a DBD contacts the major groove of the DNA at a recognized site. The other zinc finger is involved in the interaction of the heterodimer partners.

D domain

The D domain is a hinge region with a nuclear localization signal. The hinge between the DBD and LDB allows conformational changes to occur in response to ligand. The hinge provides flexibility to the proteins, allowing them to bind direct,

inverted, and everted repeat response elements. The nuclear localization signal targets the receptor to the nucleus of the cell where it will encounter DNA.

E domain

The E domain contains the ligand-binding pocket, main dimerization domain, and ligand-dependent transactivation domain called AF-2. It is a structured and conserved domain forming an antiparallel alpha-helical sandwich (Duong and Rochette-Egly, 2010). Within this structure, there is a hydrophobic cleft necessary for the binding of coregulators. Unlike the AF-1 in the AB domain, the transcriptional activity of the AF-2 is well understood. The activity of AF-2 is dependent on the integrity of the most C-terminal helix of the LBD (Rochette-Egly, 2003). In this process, the binding surface for general transcription factors is not altered by the presence of ligand on the RAR or RXR, although it is for other nuclear receptors (Bastien *et al*, 2000).

F domain

The F domain is at the C-terminal and is only present in RARs, not RXRs. Currently its function is unknown.

A/B domain

The A/B domain is located at the N-terminal and is the least conserved region. This domain accounts for the differences among RAR isoforms. It contains a ligand-independent transactivation function (AF-1). This function may be constitutive and can synergize with the AF-2 function. Due to the sequence and size variation of this domain

among isoforms, its activation capacity also varies greatly among isoforms. The variation is due to alternative splicing and promoter usage among the isoforms that may give rise to unique functions (Taneja *et al,* 1997; Rochette-Egly *et al*, 2000). Its unconserved sequence also makes it difficult to predict the secondary structure.

The induced-fit model, reviewed by Kumar and Thompson in 2003, suggests that the A/B domain is initially in a random structure due to chance interactions. When a specific binding protein is present, a conformational change occurs that induces functional activity. This model is supported by other steroid nuclear receptors like estrogen receptors and androgen receptors (Reid *et al,* 2002; Warnmark *et al*, 2001). The secondary structures that arise based on this model would be unique to the binding protein (Warnmark *et al*, 2001). The potential binding proteins may be limited by cell type or promoter context. This would account for the promoter- and cell-specific activity AF-1 demonstrates. Furthermore, the varied AF-1 activity may also contribute to different RAR effects seen in development and homeostasis.

The transcriptional activity of AF-1 can be modulated by post-translational modification, protein-protein interaction, and synergy with AF-2. The forms of post-translational modification relevant to AF-1 transcriptional activity are phosphorylation and ubiquitination.

Post-translational Modification of AF-1

Phosphorylation occurs at serine residues in proline-rich sites which are recognized by cyclin-dependent kinases (CDKs) and mitogen-activated protein kinases (MAPKs) (Morgan, 1995 and 1997; Pearson, 2001; Chang, 2001). The exact location and

number of phosphorylation sites differs by RAR or RXR subtype. Phosphorylation of the AF-1 region induces its transcriptional activity by aiding in the recruitment of coactivators and increasing chromatin decompaction. It may also stabilize the receptor-transcription complex by aiding in recruitment of transcription machinery (Rochette-Egly, 2003). Cdk7, part of TFIIH, is responsible for phosphorylation of sites in AF-1 of RARs. Other cdks phosphorylate AF-1 sites in RXRs. p38MAPK can also phosphorylate the A/B domain of RARγ, which signals ubiquitination of the receptor (Gianni *et al*, 2002; Kopf *et al*, 2000). Disruptions to the phosphorylation process, through receptor mutations, improper kinase activity, or other means, reduce the transcriptional activity of AF-1.

Ubiquitination occurs at highly conserved lysine residues to target proteins for degradation by the proteasome. Covalently attached polyubiquitin chains on proteins are recognized by the 26 S proteasome. Degradation of the DNA-bound nuclear receptors allows transcription to proceed. It also stops further transcription until another heterodimer binds to the DNA to initiate a new round of transcription. This process can occur at the AF-2 as well.

Protein-AF-1 Interactions

The effect of a protein-AF-1 interaction on transcription is dependent on the particular protein, receptor subtype, or target gene promoter. The proteins capable of interacting with RAR AF-1 include mRNA processing, chaperone, and transferase proteins in addition to general transcription factors and coregulators.

Acinus-S', a nuclear protein involved in chromatin condensation and mRNA splicing, interacts with all RAR subtypes at the A/B domain but not with other steroid/thyroid hormone superfamily members. This interaction represses AF-1 transcriptional activity, partially through HDAC activity (Vucetic *et al*, 2008). TSA treatment does not fully block the transcriptional effects of acinus-S' which indicates deacetylation is not the only method by which acinus-S' exerts its effects. Other coregulatory proteins such as CoAA and CAPER are involved in regulating transcription and mRNA processing (Auboeuf *et al*, 2004; Dowhan *et al*, 2005). Given the association of acinus-S' with mRNA-processing machinery, similar functioning may be involved in this case. The transcriptional repression occurs in a ligand-independent manner, consistent with the ligand-independent function of AF-1. The promoter context of an endogenous RAR target gene is also relevant to the acinus-S' binding effect on transcriptional activity of AF-1 (Vucetic *et al*, 2008). The promoter architecture or binding of other regulators may interfere with the binding of acinus-S' for some RAR-regulated genes which causes its effects to vary.

Vinexin β is another AF-1 interacting protein, exclusive to RARγ, which represses AF-1 transcriptional activity (Bour *et al*, 2005b). Vinexin β is a cytoskeletal protein also involved in signal transduction pathways. It has no enzymatic activity (Akamatsu *et al*, 1999). The other RAR subtypes have a transcriptionally active AF-1 when that domain is phosphorylated by cdk7, as discussed previously. RARγ requires a second phosphorylation by p38MAPK for transcriptional activity (Gianni *et al*, 2002). In the absence of phosphorylation at both of these sites, vinexin β is able to bind RARγ. The

dissociation of vinexin β from RARγ is required for AF-1 activation (Bour *et al*, 2005b). The mechanism of repression is unknown.

Synergy with AF-2

The phosphorylation of AF-1 by cdk7 activates its transcription in a ligand independent manner. Interestingly, this process may be modulated by the binding of cyclin H, another member of the THIIF complex, with AF-2 (Bour *et al*, 2005a). The cooperation of these two interactions increases the overall transcriptional activity of the RARs. The ligand-dependent recruitment of general transcription factors to the promoter allows the binding between AF-2 and cyclin H to occur (Pavri *et al*, 2005; Bour *et al*, 2005a). This, in turn, causes a conformational change of the entire RAR such that the phosphorylation site on AF-1 is exposed to cdk7 (Bour *et al*, 2005a). The result is concurrent transcriptional activation at the AF-1 and AF-2 regions. Likewise, coactivators have been shown to concurrently activate both transcriptional functions by binding to both domains (Bommer *et al*, 2002).

Ubiquitination and autonomous degradation of the receptor is dependent on ligand activation of the AF-2. It also requires heterodimerization with RXR (Kopf *et al*, 2000). The liganded receptor recruits SUG1, a DNA helicase part of the 19 S regulatory complex of the 26 S proteasome (vom Baur *et al*, 1996). Once the proteasome is present, in conjunction with a phosphorylated AF-1, the partner receptor may also be degraded (Gianni *et al*, 2003). In other words, while each partner nuclear receptor can regulate its own degradation through its AF-2, a synergistic effect with its AF-1 may cause the degradation of the heterodimerized partner.

IV. HACE1

HECT domain and Ankyrin repeat containing E3 ubiquitin-protein ligase (HACE1) was first identified as a novel open reading frame located near a translocation break point on chromosome 6q21 in a sporadic Wilms' tumor (Angelsio *et al*, 2004). It is highly expressed in normal heart, brain, pancreas, and kidney tissues. HACE1 primarily localizes to the endoplasmic reticulum and cytoplasm of cells with a small amount in the nucleus (Anglesio *et al*, 2004). HACE1 has been shown to be downregulated in 50% of primary human tumors, including T and NK cell lymphomas, central nervous system lymphomas, prostate cancers, pancreatic tumors, and ovarian carcinomas, due to aberrant methylation (Anglesio *et al*, 2004, Zhang *et al*, 2007).

HACE1 has 24 exons that encode a HECT domain linked to six ankyrin repeats. The long form of HACE1 encodes a 909 amino acid protein, and the short form encodes a 562 amino acid protein. Limited study of HACE1 short form has yielded little information on its function. It is thought to play an important role in the central nervous system due to the size of the protein, and its expression in the brain (Nagase *et al*, 2000). Unless indicated otherwise, all reference to HACE1 concerns the long form.

HECT stands for homologous to E6-AP C-terminus. The HECT domain is common to E3 ubiquitin ligases and plays a critical role in the eukaryotic ubiquitin-proteasome system. It functions by accepting an ubiquitin from an ubiquitin-conjugating protein and catalyzing its transfer to a target protein. This function is necessary for the regulation of various signal transduction pathways, protein trafficking, and DNA damage, among other cellular processes (Marin, 2010). HACE1 utilizes the E2 enzyme UbcH7 in its E3 ubiquitin ligase activity (Anglesio *et al*, 2004).

Ankyrin proteins are believed to function in the coupling of a variety of integral membrane proteins to spectrin. Ankyrin-like repeats have been detected in various regulatory proteins and are present in HACE1 in the form of six repeats. One ankyrin repeat is 33 amino acids long, and the repeats occur in at least four consecutive copies. Terminal copies have more variable sequences than those located internally. The ankyrin repeat domain plays a role in protein-protein interaction (Bork, 1993).

HACE1-deficient mice have been shown to have an increased incidence of tumors after a second hit. Spontaenous late-onset cancers occur after genetic inactivation in mice. Conversely, overexpression of HACE1 suppresses the growth rate of multiple cell lines. Due to these observations, HACE1 has been identified as a novel tumor suppressor. The E3 ubiquitin ligase catalytic cysteine mutant, HACE1 C876S, does not suppress cell growth, anchorage-independent growth on soft agar, and tumorigenicity. As such, the tumor suppressive effects of HACE1 are thought to be dependent on its ubiquitin ligase activity (Zhang *et al*, 2007).

HACE1 and RAR Interaction and Its Effects

While the majority of RAR and HACE1 protein do not colocalize, a yeast two-hybrid screen and *in vivo* coimmunoprecipitation experiments in this lab have shown there is a physical interaction between the proteins. Furthermore, this interaction has been shown to occur between the AF-1 region of RARs and the C-terminus of HACE1. HACE1 interacts with isoforms 1, 2, and 3 of RARβ, isoform 1 of RARα, and isoform 1 of RARγ. Through this interaction, HACE1 represses the transcriptional activity of RARβ and RARα in the presence of RA but not RARγ (Zhao *et al*, 2009). It is suspected

to exercise this repression through its inhibition of the RA-dependent degradation of RARβ_3. The transcriptional repression of HACE1 on RARs is not generalized to all RAR-regulated genes. RAI3 is a RAR-regulated gene whose transcription was not repressed by HACE1; presumably, there are other genes likewise unaffected (Zhao *et al*, 2009). The varied transcriptional effects of HACE1 may be due to different functions of RAR subtypes or promoter context. It has been shown previously that degradation of nuclear receptors and RA-dependent transcriptional activity are linked (Gianni *et al*, 2002).

CHAPTER 2
STATEMENT OF GOALS

The physiological effects of RA are exerted through interaction with RARs and RXRs by modulating their transcriptional activities. These receptors belong to the steroid/thyroid hormone nuclear receptor superfamily which is characterized by a common structure of five or six functionally distinct domains, termed A through F. At the N-terminus, the AB region contains a ligand-independent transactivation function (AF-1). The most conserved C region contains the DNA binding domain (DBD) characterized by a pair of zinc fingers. The D domain is the hinge region connecting domains C and E. The E domain contains a ligand-dependent transactivation function (AF-2) and a corresponding ligand binding domain (LBD). It also contains the dimerization surface and surfaces for the binding of coactivators and corepressors. The F domain, present in RARs but not RXRs, has an unknown function (Soprano *et al*, 2004). There are three subtypes of RARs each with multiple isoforms.

RARs heterodimerize with RXRs to exert transcriptional control by binding to DNA. The nuclear receptors bind to RAREs, which are present in the promoters of RA responsive genes. For the AF-2, when RA is not present, the heterodimerized receptors bound to DNA recruit corepressors and histone deacetylases for chromatin compaction to prevent transcription. In the presence of RA, corepressors unbind due to a conformational change in the LBD, and coactivators, histone acetylases, and histone methyltransferases are recruited. This causes the chromatin to be decompacted and allows for transcription machinery to access the gene for transcription to occur.

The transcriptional mechanism of the AF-1 is less understood. The A/B regions

are variable among the RARs and lack a predictable secondary structure. As such, it is important to study all RARs, when focusing on the A/B regions, to determine if there are differences in the transactivation functions of the AF-1s of the RAR subtypes. The induced fit model speculates that the RARs form functional secondary structures when interacting with specific proteins (Kumar and Thompson, 2003). Our lab previously showed the interaction of HACE1 and the A/B domain of RAR through a yeast two-hybrid screen, coimmunoprecipitation and GST pull down assays (Vucetic *et al*, 2008; Zhao *et al*, 2009).

HACE1 was first identified as a novel open reading frame located near a translocation break point on chromosome 6q21 in a sporadic Wilms' tumor (Anglesio *et al*, 2004). It has 24 exons that encode a HECT domain linked to six ankyrin repeats. The HECT domain contains the E3 ubiquitin ligase activity and plays a critical role in the eukaryotic ubiquitin-proteasome system leading to protein degradation (Marin, 2010). The ankyrin repeat domain plays a role in protein-protein interaction (Bork, 1993).

Previous studies in our lab suggested HACE1 represses the transcriptional activity of RARs in the presence of RA (Zhao *et al*, 2009). We hypothesize HACE1 represses the transcriptional activity of RARs through inhibiting RA-dependent protein degradation of RARs bound to RAREs. Our specific aims are:

1. Study the effect HACE1 has on RAR transcriptional activity,
2. If there is an effect, to determine if HACE1 mediates it through affecting protein stability of RARs.

CHAPTER 3
MATERIALS AND METHODS

I. Reagents

Retinoic Acid

Stock solutions of retinoic acid (RA) were prepared every three weeks by dissolving powdered RA in 100% ethanol to a concentration of approximately10^{-3} M. The powdered RA was a gift from Hoffman-LaRoche, Inc. in Nutley, New Jersey. The concentration of RA was determined by absorbance at 350 nm using a Beckman, Du 640 spectrophotometer. Cells were treated with RA at a final concentration of 10^{-6} M. All RA use occurred under yellow light to prevent oxidation and isomerization. In all experiments which involved RA treatment, ethanol was used as the control treatment.

Cycloheximide

Cycloheximide powder (Sigma-Aldrich, St. Louis, MO) was dissolved in 100% ethanol to a concentration of 75 mg/mL. The solution was stored as aliquots at -20°C for 1 month. Cells were treated with cycloheximide at a final concentration of 75 μg/mL.

II. Preparation of DNA Clones

PCR Cloning

A primer set consisting of a forward and reverse primer was designed to amplify the gene of interest. Each primer was about 20 base pairs in length. The forward primer started at the transcriptional start codon ATG and continued into the coding sequence of the cDNA of the gene of interest. The 5' end of the reverse primer started at the stop

codon at the 3' end of the gene of interest and continued inward toward the 5' end of the gene of interest. A unique set of primers was designed for each gene.

For the high fidelity PCR reaction, two mixtures are first made. Mixture 1 contained 100 ng plasmid DNA, 100 μM forward and reverse primers, 1 μL of each dNTP, and ddH_2O to a final volume of 50 μL. The second mixture contained 2.6 U High Fidelity Taq Polymerase (Hoffman-LaRoche Inc.) and ddH_2O to a final volume of 50 μL. The two mixtures were then combined into a PCR tube, vortexed, and spun down. The PCR program was as follows:

Preheat: 94°C for 2 min

Denaturation: 94°C for 30 sec

Annealing: 55-65°C for 1 min } × multiple cycles

Elongation: 72°C for 1 min/kb product

Final Extension: 72°C for 7 min

The temperature for the annealing step should be optimized for the specific primers in use based on G/C content. The number of cycles should be optimized for each product. When using plasmid DNA as a template, 18 cycles is usually sufficient.

The size of the product and specificity of the primers was checked by running 5 μL of the product on an agarose or polyacrylamide DNA gel. If a single band of the proper size was obtained, the PCR product was purified using a QIAquick PCR Purification Kit (Qiagen, Germantown, MD) and following the manufacturer's protocol.

Agarose Gel Electrophoresis for DNA

To determine the quality of supercoiled plasmid DNA or resolve linear DNA fragments between 0.5 kb and 10.0 kb, a 1% agarose gel was used. The gel was prepared by dissolving 0.5 g of agarose in 50 mL of TAE buffer by heating in a microwave for 1.5 minutes. Ethidium bromide was added to the warm solution prior to pouring for setting. TAE buffer consisted of 40 mM Tris, 1 mM EDTA, and 20 mM sodium acetate at pH 7.2. The electrophoresis was performed at 120 mA for 90-120 minutes in TAE. Following electrophoresis, DNA stained with ethidium bromide was visualized under UV light. The molecular weight, purity, and concentration of DNA can be estimated from this method.

Polyacrylamide Gel Electrophoresis for DNA

DNA fragments smaller than 1.3 kb were analyzed on a 10% polyacrylamide gel. The gel was prepared by mixing 3 mL of 30% acrylamide/0.8% N, N'-methylene bisacrylamide, 2 mL of 5x TBE, 4.985 mL of sterilized ddH_2O, 100 μL of 10% ammonium persulfate, and 5 μL of N, N, N', N'-tetramethylene diamine (TEMED). TBE buffer consisted of 89 mM Tris-Cl, 100 mM boric acid and 3 mM EDTA at pH 8.2. The electrophoresis was performed at 200 volts for 20-30 minutes in TBE. Following electrophoresis, gel was stained with ethidium bromide and DNA was visualized under UV light.

Restriction Enzyme Digestion

DNA was digested with a restriction enzyme to confirm its identity. The reaction for each digestion contained 1x reaction buffer which is optimized for each specific enzyme, 1 µg plasmid DNA or PCR product, 20 to 80 units of restriction endonuclease (New England Biolabs, Inc., Ipswich, MA), 1x BSA if necessary, and sterilized ddH_2O up to 50 µL total volume for each reaction. The reaction was incubated in a water bath at an optimized temperature for 2-24 hours. The products of the digestion were visualized as described above by agarose or polyacrylamide gel electrophoresis with ethidium bromide staining.

Cloning by Invitrogen Gateway System

It was necessary to clone RARα_1 and RARγ_1 in a mammalian expression vector containing a tag which would permit detection of the exogenous gene. Invitrogen (Carlsbad, CA) Gateway cloning uses the integrase/*att* site-specific recombination properties of bacteriophage lambda. This technology facilitates directional cloning of PCR products into multiple destination vectors from a single entry vector. The products involved in this system were purchased from Invitrogen and include the entry vector pCR8/GW/TOPO TA cloning kit, destination vector pcDNA3.1/nV5-DEST, and Gateway LR Clonase II enzyme mix.

The first step using this technology was to obtain a purified PCR product of the gene of interest. The primers used for this must maintain the proper reading frame and include a stop codon at the 3' end of the sequence when using an N-terminus tag. The DNA was amplified using standard PCR as described above. Gel electrophoresis was

used to verify the size of the product. The product was purified using the QIAquick PCR Purification Kit (Qiagen Inc., Valencia, CA) according to the manufacturer's protocol to remove free nucleotides and proteins in the reaction.

After obtaining a purified PCR product of the gene of interest, the next step was to insert it into the TOPO entry vector. The reaction mixture for this contained 0.5-4 µL fresh PCR product, 1 µL salt solution (1.2 M NaCl, 0.06 M $MgCl_2$), and sterilized ddH_2O up to 5 µL total volume. After mixing, 1 µL entry vector pCR8/GW/TOPO was added. The reaction was gently mixed by pipetting up and down. The reaction was incubated at room temperature for 5 minutes and then placed on ice. Two microliters of the reaction was added to one vial of thawed One-Shot Top10 chemically competent *E. coli* cells from the TOPO cloning kit and mixed by swirling the tube. The tube was incubated on ice for 5-30 minutes. The cells were heat shocked in a 42°C water bath for 30 seconds and then moved back to ice. Next, 250 µL of SOC medium was added to the cells. SOC medium contained 2% w/v tryptone, 0.5% w/v yeast extract, 10 mM NaCl, and 2.5 mM KCl in ddH_2O. After autoclaving, 20 mM glucose was added immediately prior to use. The bacterial cells were incubated at 37°C for 1 hour while shaking.

To select and grow colonies, 10 µL, 20 µL, and 50 µL of the bacteria culture was spread on three LB agar plates containing 100 µg/mL of spectinomycin. The LB agar plates contained 1% w/v tryptone, 0.5% w/v yeast extract, 0.5% NaCl, and 1.5% bactoagar. The antibiotics were added following autoclaving and cooling of the solution. Then the plates were poured. The bacteria on the plates were incubated overnight at 37°C. Several hundred colonies were visible the following day of which 2-6 were selected for overnight growth in 5 mL of LB medium. LB medium had the same

composition as the LB agar plates without the bactoagar, containing 100 µg/mL of spectinomycin. Plasmid DNA was isolated using the NucleoBond Plasmid Purification Mini Kits (Macherey-Nagel GmbH & Co. KG, Bethlehem, PA) for analysis by restriction digestion. Appropriate endonucleases were chosen that would indicate if the entry vector contained the gene of interest and if it was in the proper orientation based on band sizes seen by gel electrophoresis. The colonies were further confirmed using DNA sequence analysis performed by Genewiz (South Plainfield, NJ) using the GW1 and GW2 primers included in the TOPO cloning kit.

A destination vector was chosen for its ability to express recombinant proteins in bacterial cells using a T7 promoter and in mammalian cells using a CMV promoter. Specifically, the destination vector pcDNA3.1/nV5-DEST was chosen for its N-terminus V5 tag that allowed for efficient detection of exogenously expressed proteins with an antibody targeting V5.

Transformation into Bacterial Cells

Chemically competent *E. coli* DH5α cells were used for transformation of plasmid DNA or ligation reactions. To make chemically competent cell, the *E. coli* DH5α cells were freshly streaked on an SOB plate consisting of 2% bactotryptone, 0.5% yeast extract, 10 mM NaCl, 2.5 mM KCl, 10 mM $MgCl_2$, and 10 mM $MgSO_4$ and incubated at 37°C. The following day, these cells were inoculated in 30 mL SOB medium and incubated at 37°C with shaking for 3-4 hours. The cells were collected when the absorbance at 550 nm was 0.45-0.55. The cells were pelleted in a centrifuge at 6,800 g for 15 minutes. After aspirating off the supernatant, the cells were resuspended in 10 mL

transformation buffer (TFB) and incubated on ice for 15 minutes. TFB consisted of 10 mM K-MES pH 6.3, 45 mM $MnCl_2 \cdot 4H_2O$, 10 mM $CaCl_2 \cdot 2H_2O$, 100 mM KCl, and 3 mM $HACoCl_3$. The cells were again pelleted in a centrifuge at 6,800 g for 15 minutes. The cells were resuspended in 2.4 mL of TFB. Subsequently, 84 µL of DnD was added to the cells for a final concentration of 3.5% by volume. DnD consisted of 1 M DTT, 90% by volume DMSO, and 10 mM potassium acetate. After a 10 minute incubation on ice, 84 µL of DnD was again added to the cells for a final concentration of 7% by volume. Following final 15 minute incubation on ice, the cells were ready for transformation in 210 µL aliquots.

Four microliters of the ligation or recombination reaction was used for transformation by swirling the tube to mix it with the competent cells. Alternatively, 100 ng of plasmid DNA was used for transformation. The cells were incubated on ice for 30 minutes. Next, the cells were heat shocked at 42°C for 90 seconds and immediately quenched on ice for 2 minutes. Then, 800 µL of SOC medium was added to the cells followed by incubation at 37°C with shaking for 1 hour. Finally, the cells were spread on LB agar plates containing antibiotic and incubated at 37°C overnight.

All clones used in this study are summarized in Table 3.1.

Table 3.1: RAR and other clones used in this study.

Insert	Vector	Tag	Mammalian Expression?	Antibiotic Resistance
$RAR\alpha_1$	pcDNA 3.1/nV5-DEST	5' V5	Yes	A
$RAR\beta_3$	pcDNA 3.1/nV5-DEST	5' V5	Yes	A
$RAR\gamma_1$	pcDNA 3.1/nV5-DEST	5' V5	Yes	A
$RXR\alpha_1$	pSG5		Yes	A
RARE-luc	pTL-luc		Yes	A
Renilla	pTK-RL		Yes	A

A: ampicillin resistance

Storage of Clones

Each bacterial clone from a recently streaked plate was inoculated in 5 mL LB medium with the appropriate antibiotic and incubated at 37°C with shaking for 16 hours. One milliliter of the culture was mixed with 1 mL of 80% glycerol and stored at -20°C in a cryogenic vial.

Isolation of Plasmid DNA

Plasmid DNA was isolated using NucleoBond Plasmid Purification kit (Macherey-Nagel GmbH & Co. KG) according to the manufacturer's protocol. To obtain sufficient quantity of DNA for mammalian cell transfection, a midi prep from a 200 mL culture was normally used.

The purity of the DNA was determined by two methods. The absorbance at 260 nm and 280 nm was measured using a Nanodrop 2000 (Thermo Scientific, Waltham, MA). A 260/280 ratio greater than 1.8 indicated sufficient purity from proteins to use in further studies. The concentration of the plasmid DNA was also determined based on the A_{260} using the following calculation: concentration (μg/mL) = $A_{260} \times 50$ μg/mL. Finally, electrophoresis of the plasmid DNA on an agarose gel as previously described indicated its structure and purity from other DNA.

III. Mammalian Cell Culture

Cos7 Cell Line

The Cos7 cell line is derived from SV40 transformed CV1 cells. These cells originated from an adult male African green monkey kidney. This lab obtained this cell line from the American Type Culture Collection (ATCC, Manassas, VA).

Cell Culture

Cells were cultured in 37°C, 98% humidity, and 5% CO_2 incubators on petri dishes (Corning Inc., Corning, NY). The cells were grown in Complete Dulbecco's modified Eagle's medium (DMEM) containing 10% fetal bovine serum (Sigma-Aldrich), 2 mM L-glutamine (Invitrogen), 100 units/mL penicillin and 100μg/mL streptomycin (Mediatech Inc., Manassas, VA). Cells were passed every 3 to 4 days. First, the medium was aspirated from the dish. The cells were washed with sterile phosphate buffered saline, PBS, to remove the medium and the serum. Next, the cells were incubated in 0.05% trypsin-EDTA (Invitrogen) in PBS until they started to lift off the plate. Completed medium was added to the plate to neutralize the trypsin and the cells were removed and cell clumps broken up by repeated pipetting. Generally, one-fifth of the cells were replated in fresh medium for continued passage.

Charcoal Stripped FBS

When indicated, cells were carried on completed DMEM containing 10% charcoal stripped FBS. To make charcoal stripped FBS, a solution containing FBS, 5% w/v activated charcoal (Sigma-Aldrich), and 0.5% w/v dextran T_{70} (Pfizer, New York,

NY) was stirred for 1 hour at room temperature. It was then spun at 27,000 × g for 30 minutes in a Sorvall RC 5B Plus centrifuge (DJB Labcare Ltd., Buckinghamshire, England). The supernatant was decanted into a funnel lined with Whatman paper and collected in a Falcon tube. The serum was filtered through clean sheets of Whatman paper 2-3 times. Finally, it was filtered with a 0.2 µm bottle top vacuum filter (Corning, Inc.)

Cell Counting

After removing cells from the plate by trypsinization, an aliquot of cells was counted. Ten microliters of the diluted cell suspension was mixed with 10 µL of 0.4% trypan blue (MP Biomedicals, Solon, OH) in PBS. Of this mixture, 10 µL was added to each stage of the hemocytometer. All cells within the four-9x9 squares in each corner, which were not stained blue, were counted as living cells. The average of three separate counts was used to determine the approximate concentration of cells by the following calculation: cells/µL = average cell count ÷ 4 counted squares × 2 (dilution factor) × 9 total squares. The calculated cell concentration was used to plate a desired number on cells.

Storage and Recovery of Cell Lines

For long term storage, actively growing cells were removed by trypsinization from a plate. After counting, the cells were spun at 110g for 5 minutes at 4°C, and the medium was removed from the pellet. The cells were resuspended in cold DMSO Freeze Medium (Hoffman-LaRoche Inc.). One milliliter of freeze medium was used for every

10^6 cells. Cells were stored in cryogenic freezing vials in 1 mL aliquots and stored at -80°C for 24 hours. Finally, the vials were moved to a liquid nitrogen tank.

To recover cells from a liquid nitrogen tank, they were quickly thawed in a 37°C water bath. The cells were spun at 110 × g for 5 minutes in a sterilized falcon tube, and the freeze medium was removed from the pellet. The cells were resuspended in completed DMEM medium and moved to a 100 mm cell culture plate. After four hours, the cells were examined under a microscope to see if they attached to the plate. The next day, they were examined again for viability.

Transient Transfection

Cells were transfected with various DNAs using TransIT-LT1 Transfection Reagent (Mirus Bio LLC, Madison, WI). Cos7 cells were plated 24 hours prior to transfection so that the cells were 90% confluent at the time of transfection. For a 35-mm plate, 1.6×10^5 cells were initially plated to give the appropriate density. For plates of other sizes, this cell density was maintained by comparing the surface area of the plate. The transfection reaction worked best at a ratio of 3 μL Mirus to 1 μg of DNA. For a 35-mm plate, 4 μg or less of DNA was used. Mirus was added to 250 μL of Opti-MEM reduced serum medium (Invitrogen) in a sterilized falcon tube. It was mixed by pipetting the solution up and down. Next, the DNA was added to the solution. Again, the solution was mixed by pipetting up and down. The solution was incubated at room temperature for 15-30 minutes. The solution was added to the cells dropwise while the plate was gently swirled. The cells were placed in the incubator and allowed to grow for 24-72 hours. Transfection efficiency or protein expression could be measured after 24 hours.

Whole Cell Extract Protein Isolation

To isolate proteins from the whole cell, actively growing cells were first washed with PBS. The cells were removed from the plate by trypsinization and immediately moved to 4°C for the duration of the protein isolation. The cells were pelleted by centrifugation, washed with PBS, and pelleted again. The cells were lysed using TNE buffer containing the following protease inhibitors: 1 mM phenylmethylsulfonyl fluoride (PMSF), 0.5 μg/mL Leupeptin, 0.5 μg/mL Pepstatin A, and 0.5 μg/mL Aprotinin. The TNE buffer consisted of 0.05 M Tris-HCl pH 8.0, 0.15 M NaCl, 1% NP40, and 2 mM EDTA pH 8.0. Generally, 200 μL of lysis buffer was used for a 20 μL cell pellet. The pellets were vortexed with the lysis buffer and kept on ice for at least 30 minutes. Following another vortexing, the tube was spun at 20,200 × g in an Eppendorf Centrifuge 5417R (Eppendorf, Hauppauge, NY) for 15 minutes at 4°C. The supernatant contained the whole cell extract and was removed to another tube for short term storage at -20°C.

Measurement of Protein Concentration

The Bradford protein assay was used to determine the concentration of whole cell protein extracts. The protein was diluted 1:200 in a solution containing 795 μL of ddH_2O and 200 μL of Bradford reagent (Bio-Rad Inc., Hercules, CA). Each sample was incubated in the dark at room temperature for 5 minutes. The absorbance at 595 nm was determined using a spectrophotometer. A solution of Bradford reagent and ddH_2O, containing no protein, was used as a blank. The concentration for each sample was determined based on a previously generated bovine serum albumin protein standard curve.

IV. Transactivation Assays

Transient Transfection

Cos7 were plated 24 hours prior to transfection at 6.0×10^4 cells per well in 12-well plates. On day 2, 0.12 μg V5-RAR, 1.2 μg V5-HACE1 or V5 empty vector, 0.12 μg RARE-luc, and 0.012 μg pTK-RL plasmid DNA was transfected into cells with *Trans*IT-LT1 transfection reagent (Mirus Bio LLC) according to the manufacturer's protocol. Four hours after transfection, the medium was removed and replaced with completed DMEM containing charcoal-stripped serum. The following day, the medium was again replaced with completed DMEM containing charcoal stripped-serum and treated with 10^{-6} M RA or ethanol. The next day, the cells were lysed and luciferase activities were measured using the Dual Luciferase Assay Kit and its protocol (Promega Inc.,Fitchburg, WI).

Luciferase Vectors

RARE-luc, the firefly luciferase reporter vector, (Affymetrix Inc., Santa Clara, CA) is designed to express firefly luciferase when RAR is bound. It contains an RARE upstream of a minimal TA promoter. Its TATA box is from the Herpes simplex virus thymidine kinase (HSV-TK) promoter.

The pTK-RL vector was a gift from Dr. Barbara Hoffmn and Dr. Dan Liebermann at Temple University School of Medicine. It is used as a reporter control for transfection efficiency. It contains an HSV-TK promoter which drives expression of renilla luciferase.

Dual Luciferase Assay

An RARE firefly luciferase (RARE-luc) was used as the reporter for RAR transcriptional activity. A renilla luciferase (pTK-RL) was used as a transfection control and normalizer. The luciferase activities were measured sequentially from one sample using a Femtomaster FB 12 luminometer (Zylux Corp., Huntsville, AL). The Dual Luciferase Assay Kit (Promega, Inc.) was utilized according to its protocol.

Following transfection and RA treatment of the cells, they were washed twice with PBS. Cell lysates were prepared using 150 µL of 1× Passive Lysis Buffer (PLB) for each sample. The plates were rocked for 20 minutes at room temperature, and the cell lysates were collected.

One hundred microliters of LAR II firefly substrate was mixed with 20 µL of cell lysate. The firefly luciferase activity was read in the luminometer for 10 seconds after a 2 second premeasurement delay. Following this measurement, 100 µL of 1× Stop & Glo Reagent, diluted in Stop & Glo Buffer, was added to the sample and mixed. The renilla luciferase activity was measured by the luminometer under the same conditions.

An initial blank reading for both luciferase activities was obtained using 1× PLB as the sample. These values were subtracted from the rest of the sample values as background. The firefly luciferase activity for each sample was divided by its renilla luciferase activity. The sample treated with ethanol and containing only RAR, no HACE1, was arbitrarily set to 1 for each RAR subtype. The values were reported as relative luciferase units (RLU).

V. Western Blot Analysis

SDS-PAGE

Proteins between 30 and 100 kDa were resolved on 10% SDS-polyacrylamide gels. The running gel contained 9 mL filtered 30% acrylamide/0.8% Bis-acrylamide, 7.5 mL 4X Tris·Cl/SDS pH 8.8, 13.5 mL ddH_2O, 100 μL 10% ammonium persulfate, and 20 μL TEMED. The running gel was poured between two plates separated by spacers. The plates used to make the gel were previously cleaned with water and ethanol to avoid infrared contamination of the western blot. Ethanol was overlayed on top of the gel during polymerization to form a straight surface. The gel was allowed to polymerize for one hour at room temperature. The stacking gel contained 2.6 mL 30% acrylamide/0.8% Bis-acrylamide, 5 mL 4X Tris·Cl/SDS pH 6.8, 12.3 mL ddH_2O, 100 μL 10% ammonium persulfate, and 20 μL TEMED. After the ethanol was removed, the stacking gel was poured on top of the polymerized running gel. The comb was inserted immediately into the stacking gel to allow wells to form. The stacking gel was allowed to polymerize for 30 minutes at room temperature. Following polymerization of the stacking gel, the comb was removed, and the wells were washed with protein running buffer. The running chamber was assembled with the gel and filled with protein running buffer. The protein running buffer contained 25 mM Tris·Cl, 192 mM glycine, and 0.1% SDS pH 8.3.

Protein samples were prepared with 40 μg whole cell extract, 1X sample buffer, and d ddH_2O to make all samples equal volume. The 2X sample buffer contained 100 mM Tris pH 6.8, 200 mM dithiothreitol, 4% SDS, 0.2% bromophenol blue, and 20% glycerol. The samples were boiled for 5 minutes and briefly spun before loading onto the

gel. The gel was run at 100 volts for 1 hour. After running, the gel was removed from the plate and soaked in cold transfer buffer for 10 minutes.

Protein Transfer

An electroblotting apparatus was used to transfer the proteins from the gel onto an immobulin FL PVDF membrane (Millipore Inc, Billerica, MA). The membrane was soaked in 100% methanol for 10 minutes and then soaked in cold transfer buffer for 10 minutes with the protein gel. The transfer buffer contained 25 mM Tris, 192 mM glycine, and 20% methanol. The protein gel was placed on top of the membrane and sandwiched between two sheets of wet Whatman paper. This was placed between two wet sponges. The transfer apparatus was assembled so that the protein was closest to the black side, and the membrane was closest to the white side. The assembled sandwich was put in the tank so that the black side of the sandwich was against the black side of the holder to ensure the charge flowed in the direction necessary to move the proteins onto the membrane. The tank was filled with cold transfer buffer and an ice block. The buffer was continuously stirred while transferring at 100 volts for 1 hr.

When the transfer was complete, the membrane was rinsed in PBS. It was then incubated in blocking buffer (LI-COR Biosciences, Lincoln, NE) for 1 hr at room temperature with shaking. Alternatively, the membrane could be blocked overnight at 4°C.

Protein Detection by LI-COR Odyssey

Following blocking of the membrane, it was incubated with primary antibody diluted in blocking buffer with 0.1% Tween-20 for 1 hr with shaking. A list of primary antibodies and the dilutions used are summarized in Table 1. Next, the membrane was washed 3 times in PBS with 0.1% Tween-20 for 10 minutes each with shaking. The membrane was incubated with secondary antibody diluted in blocking buffer with 0.1% Tween-20 for 35 minutes. Finally, the membrane was again washed 3 times for 10 minutes each with PBS/ 0.1% Tween-20. The membrane was scanned face down on a LI-COR Odyssey scanner. A computer-generated image was created with the Odyssey software. This software was also used to quantify the relative expression of the detected proteins.

Generally, two primary antibodies were used for each membrane. One was to detect the protein of interest and the other was to detect a protein that serves as a loading/normalizing control. Typically, GAPDH was used as a loading/normalizing control. When using two primary antibodies, each must be raised in a different species. Two secondary antibodies raised against the species used for the primary antibodies are needed for amplification and detection of the primary antibodies. Each of these must be raised in the same species, which differs from the primary antibody species, but have different infrared dye tags. A list of secondary antibodies and the dilutions used are summarized in Table 3.2.

Table 3.2: Antibodies used for western blot analysis.

Primary Antibody	**Species**	**Dilution**	**Company and Catalog #**
GAPDH	Goat	1:500 1:3000	Santa Cruz Biotechnology Inc (Santa Cruz, CA), SC-20357 Santa Cruz, SC-48167
V5	Mouse	1:5000	Invitrogen, R96025
c-Jun	Rabbit	1:1000	Santa Cruz, SC-1694
Secondary Antibody	**Species**	**Dilution**	**Company and Catalog #**
Anti-Goat IRdye 680CW (red)	Donkey	1:10,000	LI-COR Biosciences, 926-32224
Anti-Mouse IRdye 800CW (green)	Donkey	1:10,000	LI-COR Biosciences, 926-32212
Anti-Rabbit IRdye 800CW (green)	Donkey	1:10,000	LI-COR Biosciences, 926-32213

VI. Protein Stability Assay

First, the appropriate concentration of cycloheximide to use was determined. On the first day, $1.25x10^5$ or $2.5x10^5$ actively growing Cos7 cells, representing low and high cell densities respectively, were seeded on 12-well plates. The following day, cells were treated with one concentration of cycloheximide: 0, 10, 25, 50, 75, or 100 μg/mL. Cells were also treated with 1 μL/mL ethanol to mimic treatment for exogenous protein stability assay. Twenty-four hours after treatment, cells were observed for cell death and growth. Whole cell extracts were made. Western blot analysis was used to visualize and quantify the relative expression of endogenous c-Jun at each concentration of cycloheximide and both cell densities.

Next, the appropriate time to start the treatment after transfection was determined. On day 1, $1.58x10^5$ actively growing Cos7 cells were seeded on 35-mm plates. On day 2, 1.8 μg V5-RARβ_3, 0.9 μg V5-HACE1, 0.45 μg pSG5-RXRα, and 0.045 μg RARE-luc

plasmid DNA was transfected into cells with *Trans*IT- LT1 transfection reagent (Mirus Bio LLC) according to the manufacturer's protocol. Whole cell extracts were made at 20.5, 24, 29, and 46 hours following transfection. Western blot analysis was used to visualize and quantify the relative expression of V5-RARβ_3 and V5-HACE1 over time.

Finally, the half-life of exogenous protein was determined using the conditions indicated by the previous experiments. On day 1, $1.58x10^5$ actively growing Cos7 cells were seeded on multiple 35-mm plates so that plates were ~90% confluent for transfection. Sixteen to twenty-four hours later, 1.8 μg V5-RAR, 0.9 μg V5-HACE1, 0.45 μg pSG5-RXRα, and 0.045 μg RARE-luc plasmid DNA was transfected into cells on each plate using *Trans*IT- LT1 transfection reagent and the manufacturer's protocol. RARα_1, RARβ_3, and RARγ_1 were each expressed in aV5 destination vector and used in experiments separately. Twenty-six hours after transfection, cells were treated with 75 μg/mL cycloheximide and 10^-6 M RA or ethanol from mastermixes of completed medium. Whole cell extracts were made from the plates at 0, 3, 5, 8, and 10 hrs after treatment. Western blot analysis in conjunction with LI-COR Odyssey and its software was used to visualize and quantify relative protein expression. The half-life of protein was calculated based on linear equations fit to protein expression data over time.

CHAPTER 4
RESULTS

I. Effect of HACE1 on Transcriptional Activities of RARs

To determine the effect HACE1 binding may have on RAR transcriptional activity of an RARE reporter gene construct, dual luciferase assays were performed using RARβ_3, -α_1, and –γ_1.

RARβ_3 Transactivation

In the absence of HACE1, the RA induced transcriptional activation of RARβ_3 was 3.37 +/- 0.91 fold induction compared to ethanol treated cells, which was significantly different with a p value less than 0.01. The RA induction of RARβ_3 in the presence of HACE1 was 2.24 +/- 0.68 fold compared to 0.80 +/- 0.34 fold induction in ethanol treated cells. The p value for this difference was less than 0.05. The RA induction of RARβ_3 transactivation in the presence of HACE1 was not significantly different from the induction in the absence of HACE1; however, the standard deviation is large for these measurements (Figure 4.1A). As a result, the trend showing that presence of HACE1 leads to a decrease in RARβ_3 transactivation is obscured.

RARα_1 Transactivation

In the absence of HACE1, the RA induced transcriptional activation of RARα_1 was 6.40 +/- 1.75 fold induction compared to ethanol treated cells, which was significantly different with a p value less than 0.01. The RA induction of RARα_1 in the presence of HACE1 was 4.08 +/- 2.03 fold compared to 0.70 +/- 0.17 fold induction in

ethanol treated cells. The p value for this difference was less than 0.05. The RA induction of RARα_1 transactivation in the presence of HACE1 was not significantly different from the induction in the absence of HACE1 (Figure 4.1B). Once again, the standard deviations are large, possibly obscuring the trend that RARα_1 transactivation is decreased in the presence of HACE1.

RARγ_1 Transactivation

In the absence of HACE1, the RA induced transcriptional activation of RARγ_1 was 2.80 +/- 0.23 fold induction compared to ethanol treated cells, which was significantly different with a p value less than 0.001. The RA induction of RARγ_1 in the presence of HACE1 was 1.59 +/- 0.22 fold compared to 0.71 +/- 0.08 fold induction in ethanol treated cells. The p value for this difference was less than 0.01. The RA induction of RARγ_1 transactivation in the presence of HACE1 was decreased from the induction in the absence of HACE1 with a p value less than 0.001 (Figure 4.1C).

A)

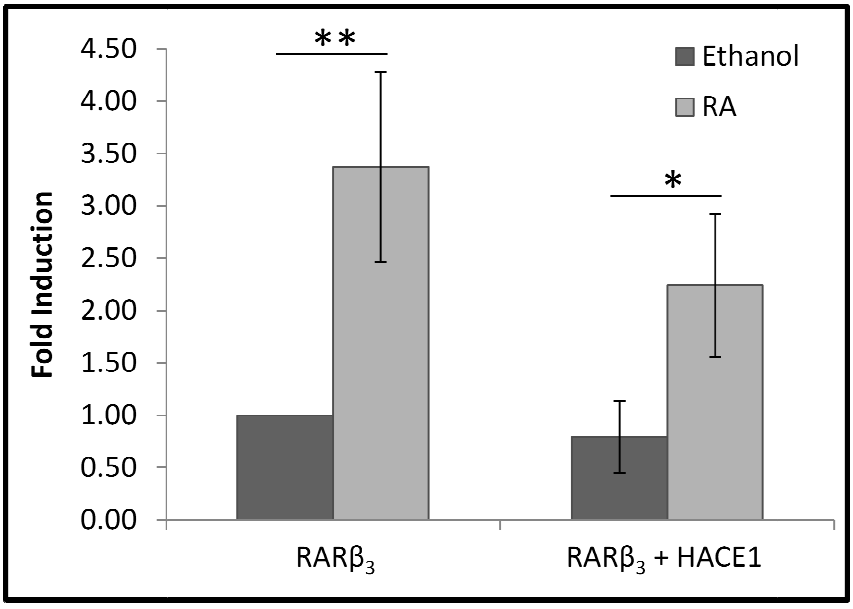

B)

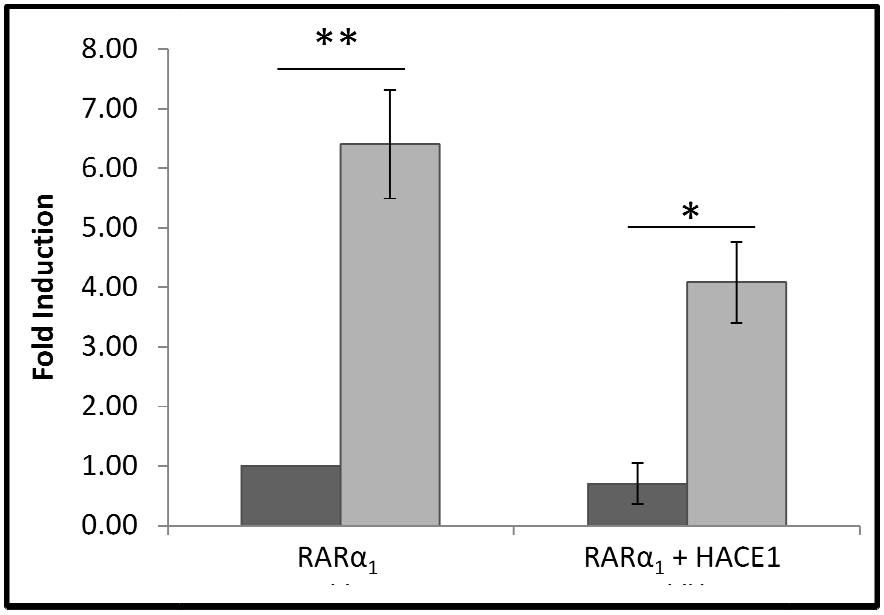

C)

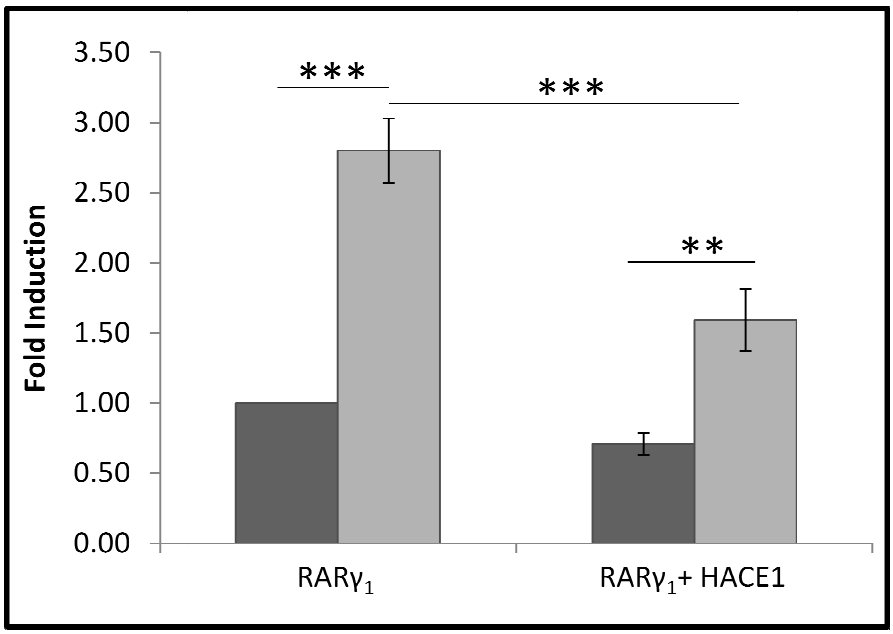

Figure 4.1: Effect of HACE1 on RAR transcriptional activity. Cos7 cells were plated at 3.3×10^4 cells/cm^2 in 12 well plates. On day two, 0.12 μg V5-RARβ$_3$ (A), V5-RARα$_1$ (B), or V5-RARγ$_1$ (C), 1.2 μg V5-HACE1 or V5 empty vector, 0.12 μg RARE-luc, and 0.012 μg pTK-RL plasmid DNAs were transfected into cells. Four hours and twenty-four

hours after transfection, the medium was removed and replaced with completed DMEM containing charcoal-stripped serum. The second time, the cells were also treated with 10^{-6} M RA or ethanol. The next day, the cells were lysed and luciferase activities were measured using the Dual Luciferase Assay Kit (Promega Inc.). Firefly luciferase values were normalized to renilla luciferase values. The ethanol treated samples in the absence of HACE1 were arbitrarily set to 1 for each RAR subtype. Fold inductions shown are the mean of three independent experiments plus or minus one standard deviation. P value was generated by Tukey-Kramer multiple comparisons test following a significant difference as determined by a repeated measures ANOVA. *: p value < 0.05; **: p value < 0.01; ***: p value < 0.001. A) RARβ_3 with and without HACE1. B) RARα_1 with and without HACE1. C) RARγ_1 with and without HACE1.

II. Development of Experimental Conditions to Examine Half-life

Optimum cycloheximide concentration and cell density

Cycloheximide stops protein translation within a cell. Its use makes it possible to determine the stability of a protein within a cell because protein degradation can be seen by western blot when cycloheximide prevents the synthesis of new proteins. Various concentrations have been reported as effective in mammalian cell culture for this purpose. The optimum cycloheximide concentration for Cos7 cells needed to be determined. Cos7 cells were plated at a density of 3.3×10^4 cells/cm^2 (low density), or 6.6×10^4 cells/cm^2 (high density). The next day, Cos7 cells were treated with 0, 10, 25, 50, 75, or 100 µg/mL of cycloheximide for 24 hours. Protein extracts from each treatment

were prepared. Expression of endogenous c-jun was visualized by western blot and quantified using LI-COR Odyssey software.

As seen in Figure 4.2, when cells were plated at low density, higher concentrations of cycloheximide inhibited translation more effectively than lower concentrations based on decreased expression of c-jun. Also, the expression level of GAPDH remained constant after 24 hours of treatment with all doses of cycloheximide. This indicated GAPDH protein was stable over 24 hours and could act as an appropriate normalizer and loading control to use for future experiments involving cycloheximide treatment. Based on observations by light microscopy, treatment with cycloheximide did not cause cell death at any of the stated doses.

Cos7 cells plated at high density did not display a dose-dependent response to cycloheximide in terms of c-jun expression (Figure 4.2). Also, basal expression of c-jun was significantly decreased at high density plating indicating conditions were not ideal for cell growth. Observations by light microscopy showed the cells were significantly overgrown on the culture dish (data not shown). For these reasons, Cos7 cells were plated at low density and treated with 75 µg/mL of cycloheximide for future experiments.

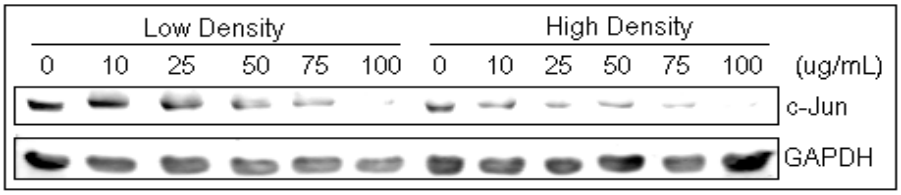

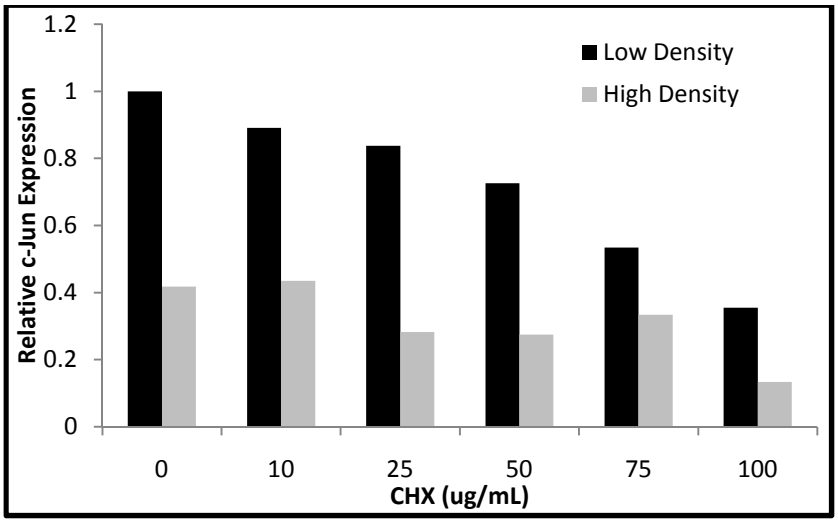

Figure 4.2: Determining optimal cycloheximide concentration and cell density for protein stability assay. Cos7 cells were plated at 3.3×10^4 cells/cm^2 (low density) or 6.6×10^4 cells/cm^2 (high density). The next day, cells were treated with 0, 10, 25, 50, 75, or 100 μg/mL cycloheximide for 24 hrs. Protein extracts were made, and endogenous c-Jun expression was determined by western blot analysis. C-Jun protein levels were quantified and normalized to GAPDH. The sample plated at low density with no cycloheximide treatment was arbitrarily set to 1.

Transfection efficiency between experiments

The experimental setup requires transfection of separate plates of cells for each time point and treatment. When isolating protein to determine its stability, it is assumed that all plates initially express the same level of protein. To determine if this is an accurate assumption, three separate transfections were performed. Western blot was used to quantify protein expression. The expression of the transfected protein, V5-RARβ_3, was consistent in each transfection (Figure 4.3).

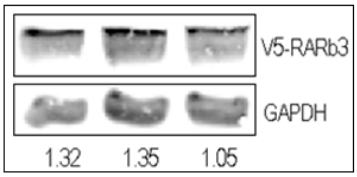

Figure 4.3: Protein expression is consistent across experiments. Cos7 cells were plated at 3.3×10^4 cells/cm^2 in 60 mm dishes. Cells were cotransfected with 4 μg V5-RARβ_3 DNA, 1 μg RXRα DNA, and 0.1 μg RARE-luc DNA from three separate mixtures. Protein extracts were made 48 hrs after transfection, and exogenous RARβ_3 expression was determined by western blot analysis. RARβ_3 protein levels were quantified and normalized to GAPDH. These values are listed below the bands.

Optimum treatment start time

In order to determine the best time to start the cycloheximide treatment, Cos7 cells were cotransfected with V5-RARβ_3 DNA and V5-HACE1 DNA. Whole cell protein extracts were isolated at 20, 24, 29.5, and 46 hours after transfection. Protein expression was determined by western blot. After normalizing to GAPDH, Figure 4.4 shows the highest levels of expression for both transfected proteins at 29.5 hours after transfection. The experimental setup requires treatment with cycloheximide to last for 8 hours. To ensure the experiment is completed while the cells are expressing the exogenous proteins at the greatest levels, the treatment was started at 26 hours after transfection (Figure 4.4).

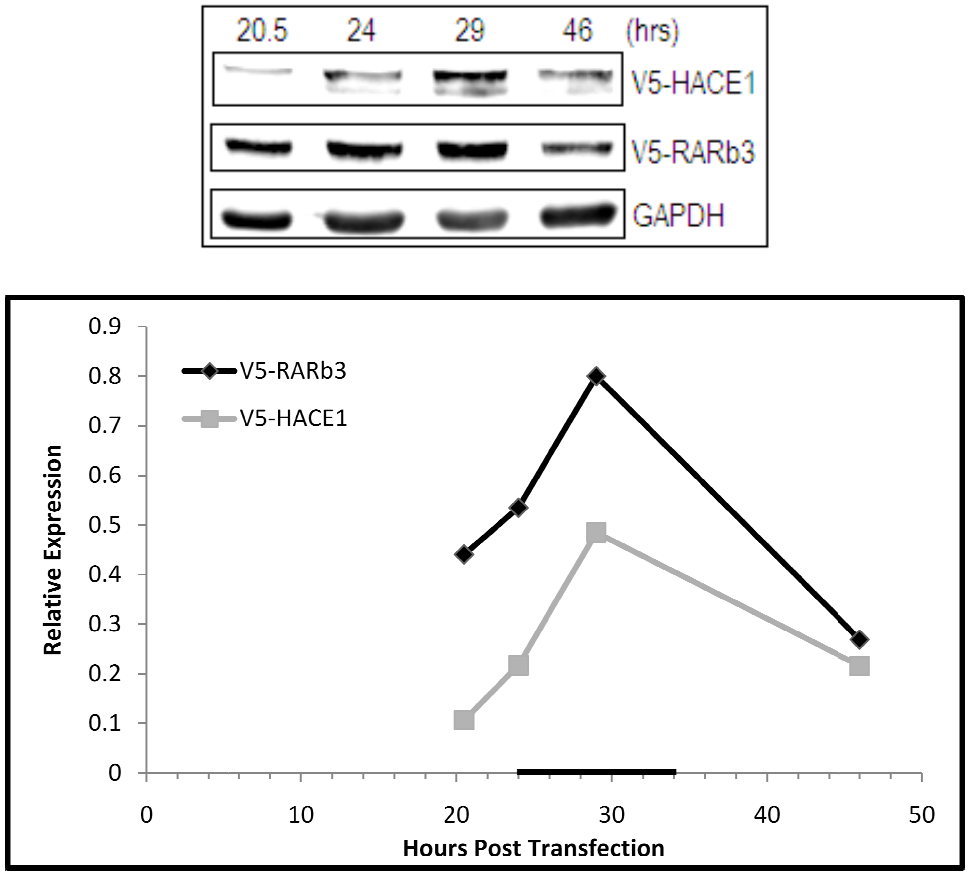

Figure 4.4: Determining optimal time to start treatment after transfection. Cos7 cells were plated at 3.3×10^4 cells/cm^2 in 35 mm dishes. Cells were cotransfected with 1.8 µg V5-RARβ_3 DNA, 0.9 µg V5-HACE1 DNA, 0.45 µg RXRα DNA, and 0.045 µg RARE-luc DNA. Protein extracts were made 20.5, 24, 29, and 46 hrs after transfection. Exogenous RARβ_3 and HACE1 expression were determined by western blot analysis. RARβ_3 and HACE1 protein levels were quantified and normalized to GAPDH. Experimental treatment time for protein stability assay is indicated by dark line on x-axis.

III. Effect of HACE1 on stability of RARs

RARs are known to be degraded by the proteasome in the presence of RA (Bour and Rochette-Egly, 2007). To determine if HACE1 affects the rate of RA dependent

degradation of RARs, the half lives of exogenous RAR proteins were determined in the presence and absence of HACE1 and with or without RA treatment. Whole cell protein extracts were isolated at 0, 3, 5, and 8 hours after inhibition of protein synthesis by cycloheximide. Western blot analysis was used to quantify the relative expression as a percentage of RAR and HACE1 from each sample (Figure 4.5A, B). The $\log_{10}$ of each percentage was plotted on a linear scale (Figure 4.5C). Linear regressions for each treatment were used to calculate the half lives. Three independent experiments were performed each for RARβ_3, RARα_1, and RARγ_1. A repeated measures analysis of variance (ANOVA) was performed for each RAR to determine if there was a statistically significant difference between any of the calculated half lives. A p value less than 0.05 was considered significant. If significance was found, a Tukey-Kramer multiple comparisons test was performed to determine between which samples the differences were found. Again, a p value less than 0.05 was considered significant.

Figure 4.5A and -B shows the relative expression of RARβ_3 and HACE1 by western blot and graph from experiment 31. HACE1 degrades over time in an RA independent manner. It degrades more slowly than all RARs. This same pattern with HACE1 is seen in all protein stability experiments and is shown here as a representation. All other experiments to determine RAR protein stability were analyzed in the same manner. To determine a linear relationship between protein expression and time, the $\log_{10}$ of the percentage of relative expression was determined and plotted. The equations of the line determined from the linear regressions listed in the table of Figure 4.5C were used to calculate the half life of RARβ_3.

A)

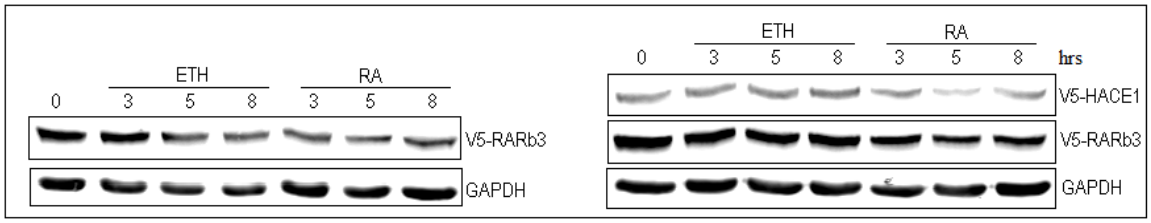
ETH
RA
0
3
5
8
3
5
8
V5-RARb3
GAPDH
ETH
RA
0
3
5
8
3
5
8
hrs
V5-HACE1
V5-RARb3
GAPDH

B)

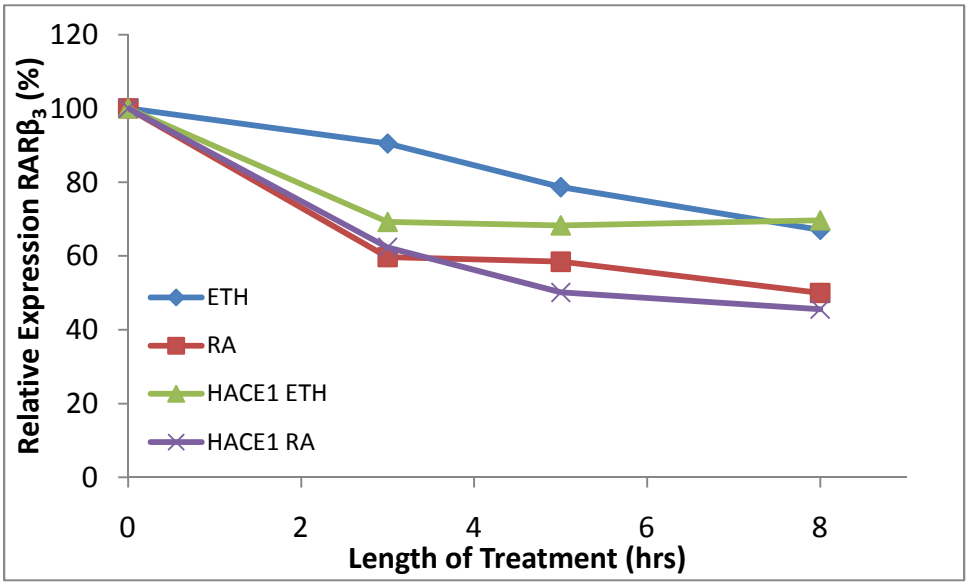
Relative Expression RARβ3 (%)
120
100
80
60
40
20
0
0
2
4
6
8
Length of Treatment (hrs)
ETH
RA
HACE1 ETH
HACE1 RA

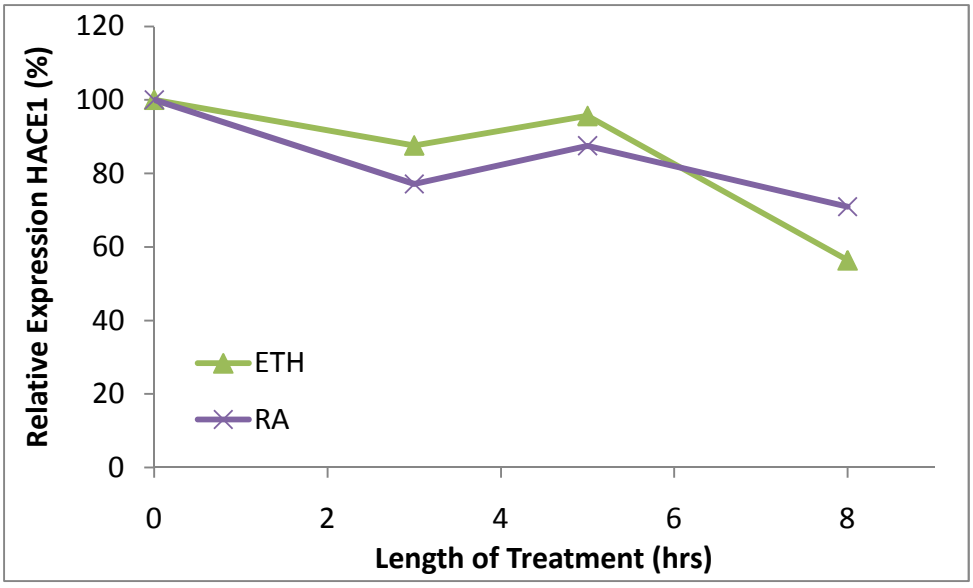
Relative Expression HACE1 (%)
120
100
80
60
40
20
0
0
2
4
6
8
Length of Treatment (hrs)
ETH
RA

C)

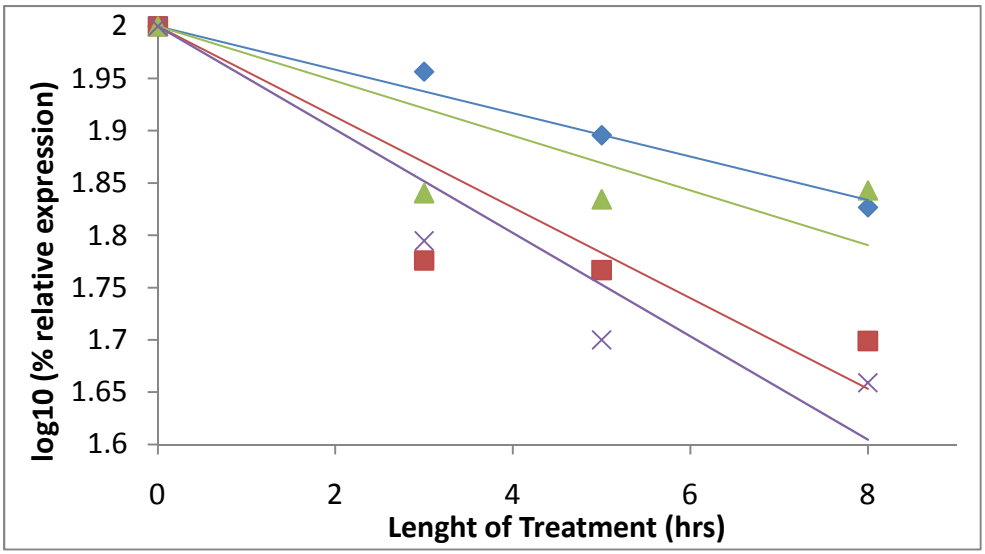

ETH	y = -0.0208x + 2
RA	y = -0.0433x + 2
HACE1 ETH	y = -0.0262x + 2
HACE1 RA	y = -0.0494x + 2

Figure 4.5: Representative RAR half life experiment 31. On day 1, Cos7 cells were plated at 3.3×10^4 cell/cm^2 in 35 mm dishes. On day 2, 1.8 µg V5-RARβ$_3$, 0.9 µg V5-HACE1, 0.45 µg pSG5-RXRα, and 0.045 µg RARE-luc plasmid DNA was transfected into cells. Twenty-six hours after transfection, cells were treated with 75 µg/mL cycloheximide and 10^{-6} M RA or ethanol. A) Protein extracts were made at 0, 3, 5, and 8 hrs after treatment, and exogenous RARβ$_3$ and HACE1 expression were determined by western blot analysis. B) RARβ$_3$ and HACE1 protein levels were quantified and normalized to GAPDH. The samples with no treatment were arbitrarily set to 100%. C) Half life of RARβ$_3$ was calculated based on linear equations generated from $\log_{10}$ of percent protein expression over time.

RARβ$_3$ Half Life

As enumerated in Figure 4.6, the mean half life of RARβ$_3$ in Cos7 cells treated with the vehicle control was 15.39 +/- 5.12 hrs (ETH). In the presence of RA, the half life was decreased in a statistically significant manner, with a p value less than 0.01, to 7.65 +/- 1.59 hrs (RA). In cells cotransfected with HACE1, the ethanol treated sample gave a half life of 11.75 +/- 3.41 hrs for RARβ$_3$ (HACE1 ETH). While falling between the determined half lives of ethanol and RA treated samples in the absence of HACE1, this half life was not determined to be significantly different from either half life in the absence of HACE1. The half life for RARβ$_3$ in RA treated cells cotransfected with HACE1 was 7.48 +/- 1.64 hrs (HACE1 RA). This was determined to be significantly different, with a p value less than 0.01, from the half life of RARβ$_3$ in ethanol treated cells in the absence of HACE1. All other comparisons were determined to be not significantly different.

Half life (hrs)					
	27	**31**	**32**	**Mean**	**SD**
ETH	10.79	14.47	20.90	**15.39**	**5.12**
RA	6.53	6.95	9.47	**7.65**	**1.59**
HACE1 ETH	8.48	11.49	15.28	**11.75**	**3.41**
HACE1 RA	7.05	6.09	9.29	**7.48**	**1.64**

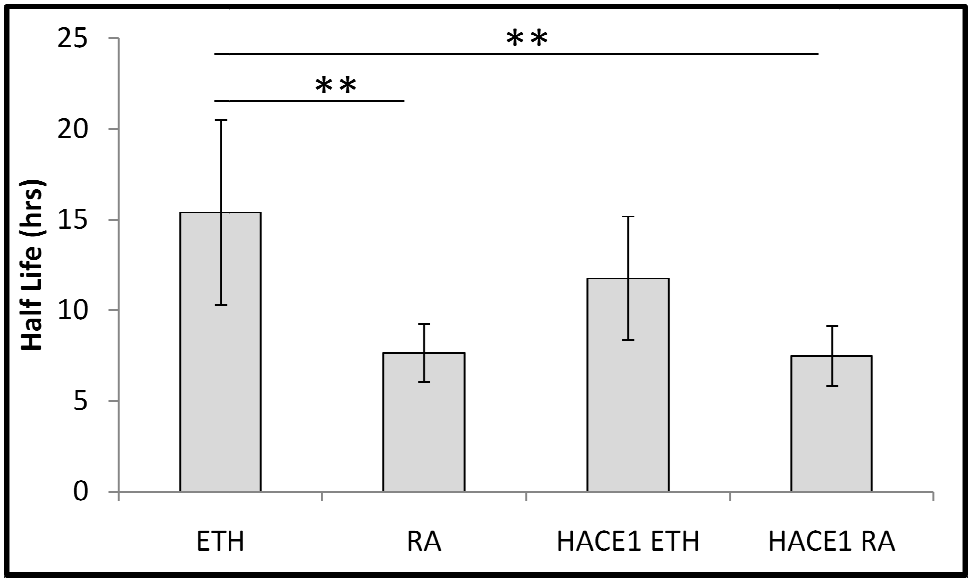

Figure 4.6: Effect of HACE1 on RARβ_3 half life. Half lives shown are the mean of three independent experiments +/- one standard deviation. P value was generated by Tukey-Kramer multiple comparisons test following a significant difference as determined by a repeated measures ANOVA. **: p value < 0.01

RARα_1 Half Life

The half life of RARα_1 in Cos7 cells treated with the ethanol was 6.95 +/- 1.09 hrs (ETH). In the presence of RA, the half life was decreased in a statistically significant manner, with a p value less than 0.01, to 4.20 +/- 0.29 hrs (RA). In cells cotransfected with HACE1, the ethanol treated sample gave a half life of 4.68 +/- 1.32 hrs for RARα_1 (HACE1 ETH). This half life was determined to be significantly different, with a p value less than 0.05, from the ethanol treated sample in the absence of HACE1. The half life for RARα_1 in RA treated cells cotransfected with HACE1 was 3.60 +/- 0.23 hrs (HACE1 RA). This was determined to be significantly different, with a p value less than 0.01,

from the half life of RARα_1 in ethanol treated cells in the absence of HACE1. All other comparisons were determined to be not significantly different (Figure 4.7).

Half Life (hrs)					
	33	**36**	**41**	**Mean**	**SD**
ETH	8.01	5.82	7.01	**6.95**	**1.09**
RA	4.04	4.02	4.53	**4.20**	**0.29**
HACE1 ETH	5.26	3.17	5.62	**4.68**	**1.32**
HACE1 RA	3.73	3.33	3.73	**3.60**	**0.23**

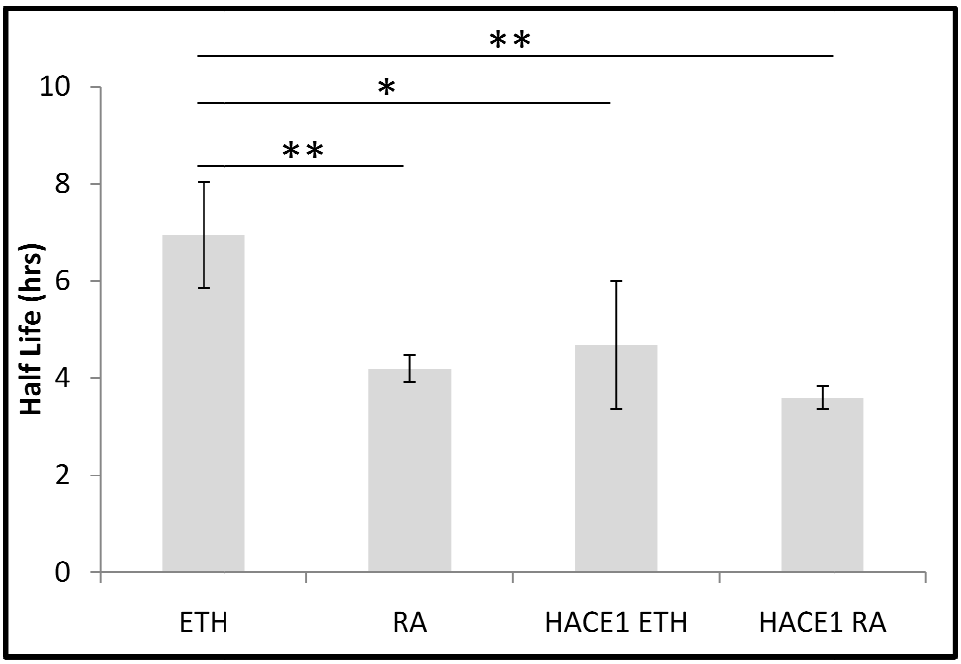

Figure 4.7: Effect of HACE1 on RARα_1 half life. Half lives shown are the mean of three independent experiments +/- one standard deviation. P value was generated by Tukey-Kramer multiple comparisons test following a significant difference as determined by a repeated measures ANOVA. *: p value < 0.05; **: p value < 0.01

RARγ_1 Half Life

The half life of RARγ_1 in Cos7 cells treated with ethanol was 7.59 +/- 1.09 hrs (ETH). In the presence of RA, the half life was decreased in a statistically significant manner to 5.07 +/- 1.01 hrs (RA) with a p value less than 0.05. In cells cotransfected with HACE1, the ethanol treated sample gave a half life of 6.38 +/- 0.70 hrs for RARγ_1 (HACE1 ETH). This half life was not determined to be significantly different from either half life in the absence of HACE1. The half life for RARγ_1 in RA treated cells cotransfected with HACE1 was 4.60 +/- 0.86 hrs. This was determined to be significantly different, with a p value less than 0.01, from the half life of RARγ_1 in ethanol treated cells in the absence of HACE1. All other comparisons were determined to be not significantly different (Figure 4.8).

Half life (hrs)						
	37	**39**	**40**	**42**	**Mean**	**SD**
ETH	8.63	6.11	7.53	8.11	**7.59**	**1.09**
RA	6.57	4.60	4.43	4.68	**5.07**	**1.01**
HACE1 ETH	5.72	6.40	5.78	7.22	**6.28**	**0.70**
HACE1 RA	3.60	4.93	4.26	5.61	**4.60**	**0.86**

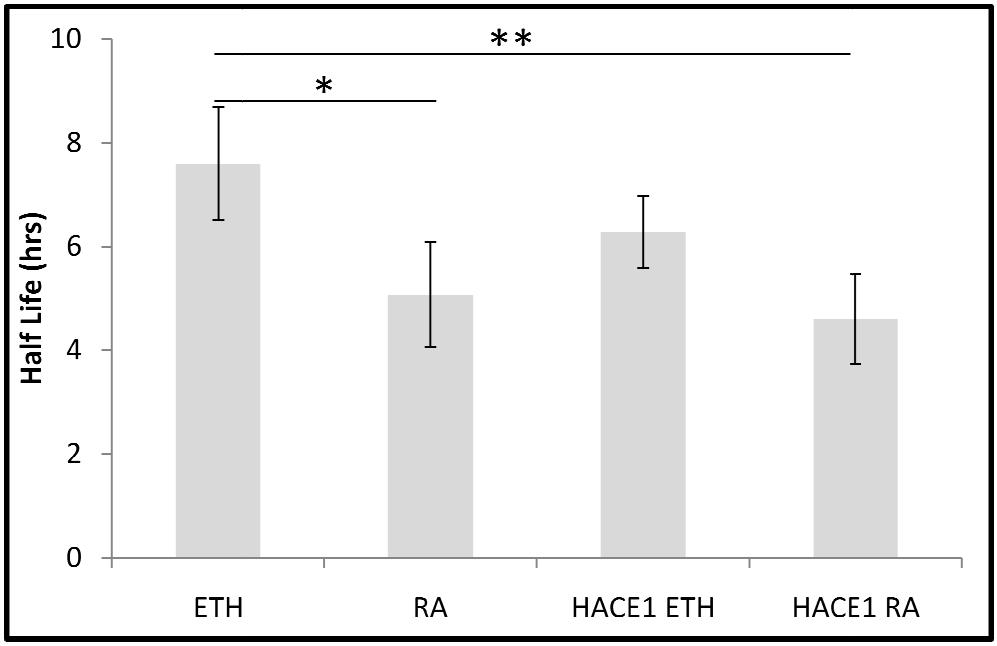

Figure 4.8: Effect of HACE1 on RARγ_1 half life. Half lives shown are the mean of three independent experiments +/- one standard deviation. P value was generated by Tukey-Kramer multiple comparisons test following a significant difference as determined by a repeated measures ANOVA. *: p value < 0.05; **: p value < 0.01

Overall, HACE1 does not appear to differentially affect the stability of RAR subtypes. With respect to RARα_1, HACE1 may slightly decrease its stability in the absence of RA. This pattern is suggested by the mean half lives for RARβ_3 and RARγ_1 as well, but does not reach the level of significance for these RAR subtypes. In the presence of RA, HACE1 does not affect the stability of any RARs allowing them to be degraded by ligand-induced proteasome recruitment in the same manner as in the absence of RA.

CHAPTER 5
DISCUSSION

The A/B domain of RARs is the least conserved region and partially accounts for the differences between RAR subtypes and isoforms (Taneja *et al*, 1997; Rochette-Egly *et al*, 2000). This domain is a candidate for the cause of different functions among RARs. Its ligand independent AF-1 may be regulated by its interacting proteins. Under this hypothesis, our lab previously performed a yeast two-hybrid screen using the A/B domain of RARβ_3 and identified multiple proteins that may interact. The proteins identified included those with functions regulating phosphorylation, methylation, and ubiquitination status of other proteins. These processes may affect the turnover or expression of RARs. Other proteins identified in the screen are involved in mRNA processing possibly affecting the transcriptional activities of RARs.

HACE1 was identified as one potential interacting protein by this method (Zhao *et al*, 2009). This interaction was confirmed by an *in vivo* coprecipitation assay. Further studies with *in vitro* GST pull-down assays showed that HACE1 also interacts with RARβ_1, -β_2, -α_1, and –γ_1. As a follow-up on these data, the overall goal of this thesis was to determine the effect of HACE1 binding on RAR transcriptional activity and a possible mechanism for its action.

Based on dual luciferase assays, HACE1 repressed transcriptional activity of RARγ_1 in the presence of RA (Figure 4.1C, 5.1A). There is a trend suggesting HACE1also repressed the transcriptional activity of RARβ_3 or RARα_1 in the presence of ligand, although large standard deviations may have obscured the statistical significance. Ligand independent repression of transcriptional activity by HACE1 was not observed to

a statistically significant degree for any RARs; however, any repression in the absence of ligand may not be apparent in this assay due to sensitivity limitations or large standard deviations of the assays.

Protein stability assays for RARα_1 showed HACE1 decreased its stability in the absence of ligand (Figure 4.7, 5.1B. The data for RARβ_3 and RARγ_1 half lives showed a trend toward this same effect, but was not statistically significant. HACE1 and RA both decreased the protein stability of RARs, but their effects are not cumulative. RA decreased the protein stability to a greater degree than HACE1 and appeared to be the dominant effector.

Taken together, these data show that HACE1 affects transcriptional activity and protein stability of RARs in a subtype specific manner. RARγ_1 transcriptional activity is repressed by HACE1 in a ligand independent manner while the other RARs may or may not be similarly affected. As a possible explanation for this repression, the effect of HACE1 on the protein stability of the RARs was compared. It has been shown previously that degradation of nuclear receptors and RA-dependent transcriptional activity are linked (Gianni *et al*, 2002). Only RARα_1 half life is affected by HACE1 in a ligand independent manner. As such, HACE1 does not appear to be repressing transcription by increasing the protein turnover of RARs in cells.

If HACE1 repressed transcriptional activity of RARs by inhibiting protein degradation, the protein stability assays would have shown that HACE1 extended the half lives of RARs regardless of ligand. The half lives in the presence of HACE1 would have been more similar to the half life of the ethanol treated sample in the absence of HACE1.

Conversely, when starting with the observation that HACE1 increased protein turnover of RARs in a ligand independent manner, the expectation for the effect HACE1 had on RAR transcription would have been opposite of what was seen. The transcriptional activity of RARs in the absence of ligand may have been comparable to the transcriptional activity in the presence of RA, if HACE1 was affecting it through altering protein stability. Alternatively, the transcriptional activity may have been abolished because the transcriptional machinery was not recruited by the ligand-bound RARs before they were degraded by HACE1.

A)

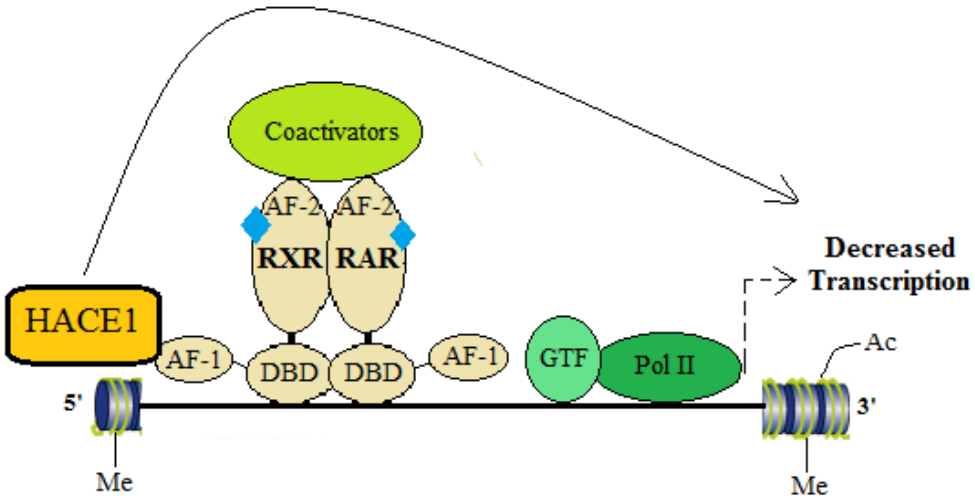

B)

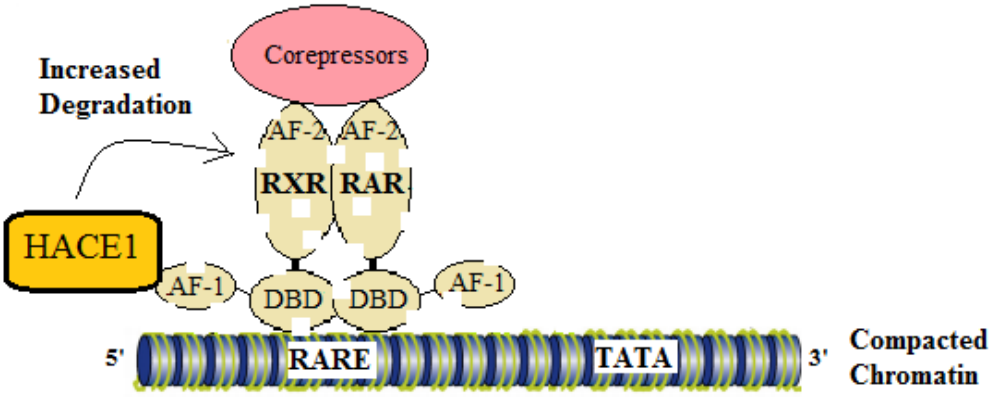

Figure 5.1: Effects of HACE1 interaction with RARs. A) Based on dual luciferase reporter assays, HACE1 inhibits RA-dependent transcription by RARs. B) Based on protein stability assays, HACE1 increases degradation of RARs in the absence of ligand.

Possible Mechanisms

The ligand dependent transcriptional repression of RARγ_1 by HACE1 may be due to the ankyrin repeat domain of HACE1. Ankyrin repeats are known to be involved in protein-protein interactions (Bork, 1993). When HACE1 is bound to RARγ_1 in the presence of ligand, it or other proteins bound to it may be sterically hindering access to the DNA by the transcriptional machinery. When vinexin β is bound to unphosphorylated RARγ, transcription is inhibited (Bour *et al*, 2005). It is unlikely that HACE1 E3 ubiquitin ligase activity is responsible for the transcriptional repression due to the binding sites of HACE1 and RARs. Our lab previously showed the C terminus of HACE1 interacts with the A/B domain of RARs (Zhao *et al*, 2009). The HECT domain, responsible for the E3 ubiquitin ligase activity, is located at the C terminus. Other characterized proteins containing a functional HECT domain interact with their substrates at the N terminal domain instead, including the eponymous E6-AP (Huang *et al*, 1999). The interaction of RARs at the C terminal of HACE1 may prevent its HECT domain from folding into the conformation needed for its function. Also, our lab previously showed that mutating the putative catalytic cysteine of the HECT domain did not affect the transcriptional repression of RARβ_3 seen in those studies (Zhao *et al*, 2009), although that transcriptional repression was not seen here.

Further supporting the negation of HACE1 E3 ubiquitin ligase activity being responsible for transcriptional repression of RARγ_1 is that the protein stability of RARγ_1 is not affected by HACE1. If HACE1 was ubiquitinating RARγ_1, the half life of RARγ_1 would most likely be decreased because it would be targeted for degradation by the 26S proteasome (Bour and Rochette-Egly, 2007).

In contrast to RARγ_1, RARα_1 is not transcriptionally repressed by HACE1. It is, however, degraded more quickly in the absence of ligand when HACE1 is present. This suggests that the E3 ubiquitin ligase activity of HACE1 may be functioning in this interaction. Given the previous evidence in literature, though, this scenario is unlikely. Again, the ankyrin repeat domain regulating protein-protein interactions may be relevant in this case with HACE1 cooperating with some unknown cofactor when bound to RARα_1. Through this method or another, HACE1 may be affecting the phosphorylation of RARα_1. The phosphorylation of the B domain was shown to be required for RARγ_2 degradation (Gianni *et al*, 2002).

Ultimately, HACE1 is a little studied protein and may have multiple functions that have not yet been deduced. Another E3 ubiquitin ligase, HERC1, acts as a guanine nucleotide exchange factor (Rosa *et al*, 1996). Cbl acts as an adaptor molecule and activates MAPKs, in addition to its E3 ubiquitin ligase function (Swaminathan and Tsygankov, 2006). The role HACE1 plays in transcription and protein degradation of RARs will require further study.

Future Directions

To further study the possible role HACE1 plays in transcriptional repression and protein instability of some RARs, the ubiquitination status of RARs in the presence and absence of HACE1 could be determined. This can be done by western blot analysis using ubiquitin specific antibodies. Similarly, the phosphorylation status could be determined using phosphorylation specific antibodies.

Previous studies in our lab overexpressed HACE1 in mammalian cells. HACE1 repressed the transcription of multiple RA regulated genes (Zhao *et al*, 2009). As a complement to these studies, HACE1 could be knocked down in mammalian cells, which may give insight into its function.

Another experiment that would expand on these results is a ChIP assay. The level of RAR bound on an RARE over time in the presence or absence of HACE1 would be expected to correlate with the degradation rate as affected by HACE1. For example, because RARα_1 was shown to degrade faster in an ethanol treated sample in the presence of HACE1, RARα_1 would be bound to the RARE for a shorter time when HACE1 is present compared to when it is not.

REFERENCES CITED

Acconcia F and Kumar R. 2006. Signaling regulation of genomic and nongenomic functions of estrogen receptors. *Cancer Lett* 238:1-14.

Akamatsu M, Aota, S, Suwa A, Ueda K, Amachi T, Yamada KM, Akiyama SK, Kioka N. 1999. Vinexin forms a signaling complex with Sos and modulates epidermal growth factor-induced c-Jun N-terminal kinase/stress-activated protein kinase activities. *J Biol Chem* 274:35933–35937.

Anglesio MS, Evdokimova V, Melnyk N, Zhang L, Fernandez CV, Grundy PE, Leach S, marra MA, Brooks-Wilson AR, Penninger J, Sorensen PH. 2004. Differential expression of a novel ankyrin containing E3 ubiquitin-protein ligase, Hace1, in sporadic Wilms' tumor versus normal kidney. *Hum Mol Genet* 13:2061-2074.

Aranda A and Pascual . 2001. Nuclear hormone receptors and gene expression. *Physiol Rev* 81:1269-1304.

Auboeuf D, Dowhan DH, Li X, Larkin K, Ko L, Berget SM, O'Malley BW. 2004. CoAA, a nuclear receptor coactivator protein at the interface of transcriptional coactivation and RNA splicing. *Mol Cell Biol* 24:442-453.

Bastien J, Adam-Stitah S, Plassat JL, Chambon P, Rochette-Egly C. 2000. TFIIH interacts with the retinoic acid receptor gamma and phosphorylates its AF-1-activating domain through cdk7. *J Biol Chem* 275:21896-21904.

Blomhoff R and Blomhoff HK. 2006. Overview of retinoid metabolism and function. *J Neurobiol* 66:606-630.

Blomhoff R, Green MH, Berg T, Norum KR. 1990. Transport and storage of vitamin A. *Science* 250:399-404.

Blomhoff R and Wake K. 1991. Perisinusoidal stellate cells of the liver: important roles in retinol metabolism and fibrosis. *FASEB J* 5:271-277.

Bommer M, Benecke A, Gronemeyer H, Rochette-Egly C. 2002. TIF2 mediates the synergy between RARalpha 1 activation functions AF-1 and AF-2. *J Biol Chem*. 277: 37961-37966.

Bork P. 1993. Hundreds of ankyrin-like repeats in functionally diverse proteins: mobile modules that cross phyla horizontally?. *Proteins* 17:363-374.

Bour G, Gaillard E, Bruck N, Lalevee S, Plassat JL, Busso D, Samama JP, Rochette-Egly C. 2005a. Cyclin H binding to the RARalpha activation function (AF)-2 domain directs phosphorylation of the AF-1 domain by cyclin-dependent kinase 7. *Proc Natl Acad Sci USA* 102:16608-16613.

Bour G, Lalevée S, Rochette-Egly C. 2007. Protein kinases and the proteasome join in the combinatorial control of transcription by nuclear retinoic acid receptors. *Trends Cell Biol* 17:302-309.

Bour G, Plassat JL, Bauer A, Lalevee S, Rochette-Egly C. 2005b. Vinexin beta interacts with the non-phosphorylated AF-1 domain of retinoid receptor gamma (RARgamma) and represses RARgamma-mediated transcription. *J Biol Chem* 280:17027-17037.

Boylan JF, Gudas LF. 1992. The level of CRABP-I expression influences the amounts and types of all-trans-retinoic acid metabolites in F9 teratocarcinoma stem cells. *J Biol Chem* 267:21486-21491.

Cañón E, Cosgaya JM, Scsucova S, Aranda A. 2004. Rapid effects of retinoic acid on CREB and ERK phosphorylation in neuronal cells. *Mol Biol Cell* 15:5583-5592.

Chang L and Karin M. 2001. Mammalian MAP kinase signaling cascades. *Nature* 410:37-40.

Chen N and Napoli JL. 2008. All-trans-retinoic acid stimulates translation and induces spine formation in hippocampal neurons through a membrane-associated RARalpha. *FASEB J* 22:236-245.

Cifelli CJ, Green JB, Green MH. 2005. Dietary retinoic acid alters vitamin A kinetics in both the whole body and in specific organs of rats with low vitamin A status. *J Nutr* 135:746-752.

Dey N, De PK, Wang M, Zhang H, Dobrota EA, Robertson KA, Durden DL. 2007. CSK controls retinoic acid receptor (RAR) signaling: a RAR-c-SRC signaling axis is required for neuritogenic differentiation. *Mol Cell Biol* 27:4179-4197.

Dilworth FJ and Chambon P. 2001. Nuclear receptors coordinate the acrivities of chromatin remodeling complexes and coactivators to facilitate initiation of transcription. *Oncogene* 20: 3017-3054.

Dollé P. 2009. Developmental expression of retinoic acid receptors (RARs). *Nucl Recept Signal* 7:e006.

Dowhan DH, Hong EP, Auboeuf D, Dennis AP, Wilson MM, Berget SM, O'Malley BW. 2005. Steroid hormone receptor coactivation and alternative RNA splicing by U2AF64-related proteins CAPERalpha and CAPERbeta. *Mol Cell* 17:429-439.

Duong V and Rochette-Egly C. 2010. The molecular physiology of nuclear retinoic acid receptors. From health to disease. *Biochim Biophys Acta* doi:10.1016/j.bbadis.2010.10.007

Everts HB, Sundberg JP, Ong DE. 2005. Immunolocalization of retinoic acid biosynthesis systems in selected sites in rat. *Exp Cell Res* 308:309-319.

Fields AL, Soprano DR, Soprano KJ. 2007. Retinoids in biological control and cancer. *J Cell Biochem* 102:886-898.

Germain P, Iyer J, Zechel C, Gronemeyer H. 2002. Co-regulator recruitment and the mechanism of retinoic acid receptor synergy. *Nature* 415:187-192.

Gianni M, Bauer A, Garattini E, Chambon P, Rochette-Egly C. 2002. Phosphorylation by p38MAPK and recruitment of SUG-1 are required for RA-induced RAR gamma degradation and transactivation. *Embo J* 21:3760-3769.

Gianni M, Tarrade A, Nigro EA, Garattini E, Rochette-Egly C. 2003. The AF-1 and AF-2 domains of RAR gamma 2 and RXR alpha cooperate for triggering the transactivation and the degradation of RAR gamma 2/RXR alpha heterodimers. *J Biol Chem* 278:34458-34466.

Green MH and Green JB. 2003. The use of model-based compartmental analysis to study vitamin A metabolism in a non-steady state. *Adv Exp Med Biol* 537:159-172.

Griffith HW. 1998. Vitamins, herbs, minerals and supplements: the complete guide. *Fisher Books*.

Gupta P, Ho PC, Huq MM, Ha SG, Park SW, Khan AA, Tsai NP, Wei LN. 2008. Retinoic acid-stimulated sequential phosphorylation, PML recruitment, and SUMOylation of nuclear receptor TR2 to suppress Oct4 expression. *Proc Natl Acad Sci USA* 105:11424-11429.

Harrison EH. 2005. Mechanisms of digestion and absorption of dietary vitamin A. *Annu Rev Nutr* 25:87-103.

Herr FM and Ong DE. 1992. Differential interaction of lecithin-retinol acyltransferase with cellular retinol binding proteins. *Biochem* 31:6748-6755.

Huang L, Kinnucan E, Wang G, Beaudenon S, Howley PM, Huibregtse JM, Pavletich NP. 1999. Structure of an E6AP-UbcH7 complex: insights into ubiquitination by the E2-E3 enzyme cascade. *Science* 286:1321-1326.

Kopf E, Plassat JL, Vivat V, de The H, Chambon P, Rochette-Egly C. 2000. Dimerization with retinoid X receptors and phosphorylation modulate the retinoic acid-induced degradation of retinoic acid receptors alpha and gamma through ubiquitin-proteasome pathway. *J Biol Chem* 275:33280-33288.

Kumar R and Thompson EB. 2003. Transactivation functions of the N-terminal domains of nuclear hormone receptors: protein folding and coactivator interactions. *Mol Endocrinol* 17:1-10.

Kurokawa R, Soderstrom M, Horlein A, Halachmi S, Brown M, Rosenfeld MG, Glass CK. 1995. Polarity-specific activities of retinoic acid receptors determined by a co-repressor. *Nature* 377:451-454.

Lee MS, Kliewer SA, Provencal J, Wright PE, Evans RM. 1993. Structure of the retinoid X receptor alpha DNA dinbind domain: a helix required for homodimeric DNA binding. *Science* 260:1117-1121.

Lee MY, Jung CH, Lee K, Choi YH, Hong S, Cheong J. 2002. Activating transcription factor-2 mediates transcriptional regulation of gluconeogenic gene PEPCK by retinoic acid. *Diabetes* 51:3400-3407.

Lefebvre P, Martin PJ, Flajollet S, Dedieu S, Billaut X, Lefebvre B. 2005. Transcriptional activities of retinoic acid receptors. *Vitam Horm* 70:199-264.

Leid M, Kastner P, Lyons R, Nakshatri H, Saunders M, Zacharewski T, Chen JY, Staub A, Garnier JM, Mader S, Chambon P. 1992. Purification, cloning, and RXR identity of the HeLa cell factor with which RAR or TR heterodimerizes to bind target sequences efficiently. *Cell* 68:377-395.

Marin I. 2010. Animal HECT ubiquitin ligases: evolution and functional implications. *BMC Evol Biol* 10:56.

Masia S, Alvarez S, de Lera AR, Barettino D. 2007. Rapid, nongenomic actions of retinoic acid on phosphatidylinositol-3-kinase signaling pathway mediated by the retinoic acid receptor. *Mol Endocrinol* 21:2391-2402.

Morgan DO. 1995. Principles of CDK regulation. *Nature* 374:131-134.

Morgan DO. 1997.Cyclin-dependent kinases: engines, clocks, and microprocessors. *Annu Rev Cell Dev Biol* 13:261-291.

Nagase T, Kikuno R, Ishikawa K, Hirosawa M, Ohara O. 2000. Prediction of the coding sequences of unidentified human genes. XVII. The complete sequences of 100 new cDNA clones from brain which code for large proteins in vitro. *DNA Res* 7:143-150.

Nagy NE, Holven KB, Roos N, Senoo H, Kojima N, Norum KR, Blomhoff R. 1997. Storage of vitamin A in extrahepatic stellate cells in normal rats. *J Lipid Res* 38:645-658.

Narlikar GJ, Fan HY, Kingston RE. 2002. Cooperation between complexes that regulate chromatin structure and transcription. *Cell* 108:475-487.

Nettles KW and Green GL. 2005. Ligand control of coregulator recruitment to nuclear receptors. *Annu Rev Physiol* 67:309-333.

Pavri R, Lewis B, Kim TK, Dilworth FJ, Erdjument-Bromage H, Tempst P, de Murcia G, Evans R, Chambon P, Reinberg D. 2005. PARP-1 determines specificity in a retinoid signaling pathway via direct modulation of mediator. *Mol Cell* 18:83-96.

Pearson G, Robinson F, Beers Gibson T, Xu BE, Karandikar M, Berman K, Cobb MH. 2001. Mitogen-activated protein (MAP) kinase pathways: regulation and physiological functions. *Endocr Rev* 22:153-183.

Quadro L, Hamberger L, Colantuoni V, Gottesman ME, Blaner WS. 2003. Understanding the physiological role of retinol-binding protein in vitamin A metabolism using transgenic and knockout mouse models. *Mol Aspects Med* 24:421-430.

Reid J, Kelly SM, Watt K, Price NC, McEwan IJ. 2002. Confomrational analysis of the androgen receptor amino-terminal domain involved in transactivation. Influence of structure-stabilizing solutes and protein-protein interactions. *J Biol Chem* 277:20079-20086.

Reijntjes S, Gale E, Maden M. 2004. Generating gradients of retinoic acid in the chick embryo: Cyp 26 expression and a comparative analysis of the Cyp 26 enzymes. *Dev Dyn* 230:509-517.

Rochette-Egly C. 2003. Nuclear receptors: integration of multiple signaling pathways through phosphorylation. *Cell Signal* 15:355-366.

Rochette-Egly C, Plassat JL, Taneja R, Chambon P. 2000. The AF-1 and AF-2 activating domains of retinoic acid receptor-alpha (RARalpha) and their phosphorylation are differentially involved in parietal endodermal differentiation of F9 cells and retinoid-induced expression of target genes. *Mol Endocrinol* 14:1398-1410.

Ronne H, Ocklind C, Wiman K, Rask L, Obrink B, Peterson PA. 1983. Ligand-dependent regulation of intracellular protein transport: effect of vitamin A on the secretion of the retinol-binding protein. *J Cell Bio* 96:907-910.

Rosa JL, Casaroli-Marano RP, Buckler AJ, Vilaro S, Barbacid M. 1996. p619, a giant protein related to the chromosome condensation regulator RCC1, stimulates guanine nucleotide exchange on ARF1 and Rab proteins. *Embo J* 15:4262-4273.

Rosenfeld MG, Lunyak W, Glass CK. 2006. Sensors and signals: a coactivator/corepressor/epigenetic code for itegrating signal-dependent programs of transcriptional response. *Genes Dev* 20:1405-1428.

Soprano DR, Qin P, Soprano KJ. 2004. Retinoic acid receptors and cancers. *Annu Rev Nutr* 24:201-221.

Swaminathan G and Tsygankov AY. 2006. The Cbl family proteins: ring leaders in regulation of cell signaling. *J Cell Physiol* 209:21-43.

Taneja R, Rochette-Egly C, Plassat JL, Penna L, Gaub MP, Chambon P. 1997. Phosphorylation of activation functions AF-1 and AF-2 of RAR alpha and RAR gamma is indispensable for differentiation of F9 cells upon retinoic acid and cAMP treatment. *Embo J* 16:6452-6465.

vom Baur E, Zechel C, Heery D. Heine MJ, Garnier JM, Vivat V, Le Douarin B, Gronemeyer H, Chambon P, Losson R. 1996. Differential ligand-dependent interactions between the AF-2 activating domain of nuclear receptors and the putative transcriptional intermediary factors mSUG1 and TIF1. *EMBO J* 15:110-124.

Vucetic Z, Zhang Z, Zhao J, Wang F, Soprano KJ, Soprano DR. 2008. Acinus-S' represses retinoic acid receptor (RAR)-regulated gene expression through interaction with the B domains of RARs. *Mol Cell Biol* 28:2549-2558.

Warnmark A, Wikstrom A, Wright AP, Gustafsson JA, Hard T. 2001. The N-terminal regions of estrogen receptor alpha and beta are unstructured in vitro and show different TBP binding properties. *J Biol Chem* 276:45939-45944.

Zhang L, Anglesio MS, O'Sullivan M, Zhang F, Yang G, Sarao R, Mai PN, Cronin S, Hara H, Melnyk N, Li L, Wada T, Liu PP, Farrar J, Arceci RJ, Sorensen PH, Penninger JM. 2007. The E3 ligase HACE1 is a critical chromosome 6q21 tumor suppressor involved in multiple cancers. *Nat Med* 13:1060-1069.